

Reviewer #1

General Comment: This paper compares surface air temperatures over China from observations and many atmospheric analyses, and seeks to improve understanding of biases in terms of deficiencies in the representation of forcing factors in the assimilating models used by the analyses. It shows that the effects of homogenising the observations are small compared with the differences between the analyses and the observations. It merits publication, but requires improvement to the presentation and discussion of results.

Response: Thanks for your high recommendation of our submission. Following your and Comment#2 constructive suggestions, the revised manuscript has been sent out for Professional English editing and we have carefully checked the revised paper and made the logic of Abstract concise and the logic of the revised paper smooth. Especially, we re-edited the Sections Discussion and Conclusions to make them clearer. We re-plotted new Fig. 3 to be more readable for readers. Below please find our point to point response to your comments.

Specific Comments:

1)

Comment: The language is generally clear, but needs a little sub-editorial refinement.

Response: Thanks, the manuscript has been sent out for Professional English editing and we have carefully made some language editing in the revised paper.

2)

Comment: Page 3, lines 44 to 50. ERA-20CM uses a newer version of the ECMWF model and sea-surface temperature analyses that are more homogeneous over time than ERA-Interim. The comparability of its pattern of trend biases with that of ERA-Interim cannot solely or necessarily be ascribed to its use of an ensemble technique. Note also that ERA-20CM used perturbed sea-surface temperature analyses, and did not include perturbations of the prescribed CMIP5 forcing. As such, classifying its approach as a “perturbed physical ensemble technique” does not seem appropriate.

Response: Thanks for your providing such information.

ERA-20CM includes the same forcing as CMIP5, please see Table 1 and website <https://www.ecmwf.int/en/forecasts/datasets/reanalysis-datasets/era-20cm-model-integrations>.

We revised it in the Abstract: The use of the ensemble technique adopted in the twentieth-century atmospheric model ensemble ERA-20CM significantly narrows the

uncertainties associated with regional warming in reanalyses (standard deviation=0.15 °C/decade).

The detailed evidence was added in the Section Discussion: Although it does not incorporate surface air temperature observations, ERA-20CM presents a pattern (with a mean of -0.04 °C/decade and a standard deviation of 0.15 °C/decade; Figs. 5 and 8) that is comparable to those of ERA-Interim and JRA-55 and **better than that of ERA-20C (mean of -0.08 °C/decade and standard deviation of 0.20 °C/decade; Figs. 5 and 8), which uses the same forecast model as ERA-20CM.** These results imply that ensemble forecasting could be used to meet important goals. **The ensemble forecasting technique used in ERA-20CM also displays advantages in that** it yields an improved simulated pattern of biases in the trends in R_s (SD=1.84 Wm⁻²/decade, 171%), precipitation frequency (SD=2.78days/decade, 122%) and L_d (SD=1.25 W m⁻²/decade, 82%) (Fig. 8).

3)

Comment: Page 4, line 58. Satellites should be included in the list.

Response: Added as suggested: ...from a variety of sources, such as surface stations, ships, buoys, radiosondes, airplanes **and satellites.**

4)

Comment: Page 4, line 66. The models used to produce reanalyses do more than fill gaps in observations.

They are important for the quality control and bias adjustment of observations, which is especially important when merging the information provided by many different types of observation.

Response: Thanks for your providing such information, which was added in the lines 96-104 of the revised paper: These reanalyses produce global gridded datasets that cover multiple time scales and include a large variety of atmospheric, oceanic and land surface parameters, many of which are not easily or routinely observed but are dynamically constrained by large numbers of observations from multiple sources assimilated using fixed NWP models. During the data assimilation, prior information on uncertainties in the observations and models are used to perform quality checks, to derive bias adjustments and to assign proportional weights. Therefore, such reanalyses add value to the instrumental record through their inclusion of bias adjustments, their broadened spatiotemporal coverage and their increased dynamical integrity or consistency.

5)

Comment: Page 5, lines 83 to 92. MERRA-2 should be included in this list.

Response: Added as suggested: ...and the National Aeronautics and Space Administration, the Modern-Era Retrospective Analysis for Research and Applications (MERRA) (Rienecker et al., 2011) **and its updated version, MERRA-2 (Reichle et al., 2017).**

6)

Comment: Page 8, line 150, and in later places, including the labelling of figures. It is wrong to label the century-scale analyses that assimilate only surface pressure (and perhaps surface wind) observations as “climate quality” compared with the shorter “NWP” reanalyses that assimilate comprehensive sets of observations. Climate quality is something that has to be demonstrated, and is not just a matter of the type of reanalysis that is carried out. The ERA-Interim and JRA-55 “NWP” reanalyses give the best climate trends for surface air temperature, as the paper shows over China. The century-scale reanalyses still suffer from changes in observations over time, as the number of surface pressure and wind observations has increased enormously over the past one hundred or more years. Also, these reanalyses use sea surface temperature and sea ice analyses that depend on observations that have changed over time. Moreover, their avoidance of upper-air observations means that their climatological states are more subject to model biases than in “NWP” analyses in which observations help determine these states. The term “climate quality” should not be used to categorize some of the reanalyses for which results are presented.

Response: Thanks for your comments. Following the BAMS paper of Dee et al., (2014), we labeled them as ‘**NWP-like reanalysis**’ and ‘**Climate reanalysis**’ in the revised paper and all the figures.

Reference: Dee, D. P., M. Balmaseda, G. Balsamo, R. Engelen, A. J. Simmons, and J. N. Thépaut, 2014: Toward a consistent reanalysis of the climate system. *Bull. Am. Meteorol. Soc.*, 95, 1235-1248.

7)

Comment: Page 10, lines 184 to 192. It would be helpful for the reader to be informed how many of the 2200 or so stations provide data that are exchanged globally under the auspices of WMO. ERA-Interim and JRA-55 analyse surface air temperature data from those stations for which data are transmitted internationally, and perhaps some additional data to which they have access for early years, but data from a significant fraction of the 2200 or so stations were probably not used by these reanalyses. It would also be helpful to know whether the observational data used in this study are publicly available to anyone who might wish to carry out such a study, or for use in future reanalyses.

Response: Data at approximately 2400 stations are conditionally exchanged with the China Meteorological Administration, publicly unavailable. Since 1961, only 194 out of approximately 2400 stations are for global exchange (please see: http://data.cma.cn/en/?r=data/detail&dataCode=SURF_CLI_CHN_MUL_DAY_CES_V3.0). This information was added in the line 196.

Note also that 824 out of approximately 2400 stations should be downloaded for the China Meteorological Administration for certain usage (http://data.cma.cn/data/cdcdetail/dataCode/SURF_CLI_CHN_MUL_DAY_V3.0.htm, in Chinese).

8)

Comment: Page 11, line 213 and pages 47 and 48. Table 1 needs some correction and tidying up. ERA-20CM did not use a 4D-VAR assimilation system as it was an ensemble of model runs. It used prescribed sea surface temperature and sea-ice analyses, but they were not produced by 4D-VAR. One column is headed “Related assimilated surface observations”, but the entry for ERA-Interim includes reference to upper-air observations, and that for MERRA-2 includes reference to aerosol observations that are not surface ones. It is stated that ERA-Interim assimilated “land surface temperature” data. It did not. It did analyse “surface air temperature data over land”, which is not the same variable. As discussed below in comment (10) it is probably better to refer to these data as analysed not assimilated.

Response: Thanks for your providing such information. We revised the main text and tidied up Table 1.

In Table 1, we corrected the column head ‘Related Assimilated Surface Observations’ as ‘**Related Assimilated and Analysed Observations**’, ‘land surface temperature’ as ‘**near-surface air temperature**’ in ERA-Interim, ‘4D-VAR’ as ‘**3D-VAR**’ in ERA-20CM and so on. For most surface observations in reanalysis, we used ‘**analysed**’ instead of ‘assimilated’ where appropriate in the revised paper.

9)

Comment: Page 11, line 222. Surface pressure observations are not distributed homogeneously in space or (especially) time. Also, sea surface temperature and sea ice analyses are not of homogeneous quality, due to observational changes. See also comment (6).

Response: Thanks for your suggestion. We corrected it as ‘relatively effective’.

10)

Comment: Pages 12 and 13, lines 246 to 251. The explanation of what ERA-Interim

and JRA-55 do could be clearer. A background surface air temperature, at a height of two metres, is produced using a processing of the model-level background forecast with the help of Monin-Obukhov similarity profiles. The observations of surface air temperature are then analysed using a relatively simple analysis scheme. It is best not to use the word assimilated as the two-metre temperatures do not affect the starting atmospheric state for the next background forecast. But they are not simply postprocessed products either – in contrast to the products from other reanalyses. Some information is retained (assimilated) in that where appropriate the increments in surface temperature and corresponding ones in relative humidity are used to update soil temperature and humidity, and these do carry over into the next background forecast. It is nevertheless probably better to refer to the observations as analysed rather than assimilated.

Response: Thanks for your providing valuable information, which was added in lines 260-264: However, the T_a in ERA-Interim and JRA-55 are post-processing products by a relatively simple analysis scheme between the lowest model level and the surface and are analysed using ground-based observations of T_a , with the help of Monin-Obukhov similarity profiles...

11)

Comment: Page 18, line 375. The better performance of ERA-Interim and JRA-55 is described as “mainly due to the post-processing of assimilated surface air temperature”. If this statement is retained it should read “mainly due to their analysis of surface air temperature data”, as discussed in comment (10). The statement is probably correct, but do the authors have evidence that this is the case? Perhaps ERA-Interim and JRA-55 simply have a better background forecast of surface air temperature due to other aspects of their data assimilation system. If the statement is to be retained, it needs to be backed up by showing that the background forecast surface air temperatures from ERA-Interim and JRA-55 are not significantly better than the surface air temperatures from the other reanalyses. In that case, analysing the surface air temperature observations must be the main reason they provide a better product.

Response: Corrected in the revised paper as suggested: perhaps due to their analysis of surface air temperature observations in ERA-Interim and JRA-55 (Table 1).

12)

Comment: Page 19, lines 383-385. It should be noted that CERA-20C used a newer model cycle than ERA-20C, and some problems that were found to affect ERA-20C were fixed in CERA-20C. So CERA-20C’s better performance than ERA-20C cannot be ascribed entirely to the use of a coupled forecast model and data assimilation.

Response: Thanks for your information, and we added such information in the revised paper: **perhaps related to** the inclusion of coupled climate forecast models and data assimilation, as well as the assimilation of surface pressure data in CERA-20C (Fig. 3 and Table 1).

13)

Comment: Page 19, line 389. The type of analysis presented in section 3.3 needs to be interpreted carefully when it comes to ERA-Interim and JRA-55. This is because their surface air temperature products involve analyses of surface air temperature observations, and values depend on the analysis increments to the background as well as to contributions via the background forecasts from key physical factors that influence surface air temperature. For example, the sentence in lines 475 to 477 on page 23 reads as if the trend biases in surface air temperature have contributions from biases in various physical forcings. But in ERA-Interim and JRA-55 such biases in physical forcing will tend to be counterbalanced by the changes the observations bring to the background forecasts. The balancing will not be perfect, so ERA-Interim and JRA-55 may inherit some of the deficiencies in forcing, but these deficiencies are likely to be much weaker than would be the case if surface air temperature observations had not been analysed.

Response: Thanks for your information, and we added such information in the end of **Section 3.4:** Note also that the incorporation of the observed changes in surface air temperatures in ERA-Interim and JRA-55 may introduce biases into the trends in the output T_a values; however, the use of partial correlation and regression analysis would lead to smaller impacts of the biases in these physical variables in quantifying their contributions to the trends in T_a .

14)

Comment: Pages 21 and 22, lines 443 to 445. Again (see comment (11)) it is asserted that the better performance of ERA-Interim and JRA-55 is due to the assimilation [analysis] of surface air temperature [observations]. This is almost certainly part of the story, but unlikely to be the only reason these two reanalyses perform better than the others. A phrase such as “in part, at least,” is needed after the word “due”.

Response: Corrected as suggested.

15)

Comment: Page 28, line 28. It is stated that ”only vegetation is included as climatology”. This is wrongly worded. Perhaps the authors mean “vegetation is only included as [a] climatology”. A number of fields other than vegetation are specified climatologically.

Response: Corrected as suggested in the lines **623-625**: In the reanalyses, vegetation is **only included as climatological information**, but the vegetation displays a growth trend during the study period of 1979-2010 within China (Fig. S23).

16)

Comment: Page 29, lines 607 to 614. I simply do not understand this paragraph.

Response: We revised this paragraph: We consider the degree to which the ensemble assimilation technique can improve the spatial patterns of the biases in the trends in Ta in the reanalyses. We find that this technique can detect the biases in the trends in Ta **over more another approximately 12% (8%)** of the grid cells in CERA-20C, which incorporates 10 ensemble members (NOAA 20CR2vc and NOAA 20CR2v employ 56 ensemble members) (Figs. 5 l-n). However, the biases in the trends in Ta over these grid cells are not significant at a significance level of 0.05, according to Student's t-test, implying that the ensemble assimilation technique cannot explain the spatial pattern of the biases in the trends in Ta identified in this study (in Figs. 5 l-n).

17)

Comment: Pages 29 to 30, lines 615 to 626. It is misleading to label the models used for the century-scale reanalyses "climate models" and the models used for shorter reanalyses "NWP models". The same ECMWF models are used for the two types of reanalysis, apart from a tendency for more recent reanalyses to use newer model versions.

Response: Thanks for your comments. Following the BAMS paper of Dee et al., (2014), we labeled them as '**NWP-like reanalysis**' and '**Climate reanalysis**' in the revised paper and all the figures.

Reference:

Dee, D. P., M. Balmaseda, G. Balsamo, R. Engelen, A. J. Simmons, and J. N. Thépaut, 2014: Toward a consistent reanalysis of the climate system. *Bull. Am. Meteorol. Soc.*, 95, 1235-1248.

18)

Comment: Page 30, lines 629. The reference to ERA-20CM is incorrect, as its circulation is not controlled by pressure data. No meteorological observations are assimilated in ERA-20CM.

Response: Thanks for your good comment and we corrected it in lines **675-677**: In ERA-20CM, the atmospheric circulation patterns are influenced by SSTs and sea ice and then partly mediate the influence of global forcings on the trends in T_a .

19)

Comment: Page 32, line 682. High temporal resolution in situ and satellite observations of precipitation are available only for recent years, so their use in reanalysis to refine trend estimates will be limited until longer time series of observations have been accumulated.

Response: Thanks for your comment. We delete this part.

20)

Comment: Page 33, lines 690 to 692. See comment (2) regarding the nature of the perturbations applied in ERA-20CM.

Response: Thank you very much. Please see Comment #2.

21)

Comment: Page 33, line 704. It is not clear why the Argo system is mentioned here, as it is not primarily an observing system for SST and sea ice, and data have been available in substantial numbers for little over a decade, posing a problem for homogeneity.

Response: Thanks for your comment. We delete it.

Reviewer #2

General Comment: The study attempts to assess the value of various global reanalysis products over the Chinese domain by comparison to a homogenized set of station data. The overall approach is logical. The findings with regards to which reanalyses products are high quality are in line with existing understanding. Some effort to understand the potential thermodynamic and boundary condition causes of differences are interesting and novel although could be presented much more simply. It is clear that a huge amount of effort has been undertaken to access and analyse a wealth of data. As such, the authors are to be commended on a substantive body of work. However, I have some concerns around aspects of the analysis and presentation. The work may be publishable in ACP following revisions if they satisfactorily address my concerns.

Response: Thanks for your effort to evaluate our submission and high recommendation. Below please find our point to point response to your comments.

Specific Comments:

1)

Comment: Treatment of observations

The main issue with the analysis is the treatment of a single homogenized series of temperature observations as constituting a ‘truth’ against which it is possible to make definitive resulting assessments of the reanalyses products. In reality no single approach to homogenization of observations can ever yield a perfect reconstruction of the true evolution of the observed variable. Therefore the observations even after homogenization cannot be treated as a demonstrable truth against which definitive statements of reanalysis quality can be made. In cases where offsets between the observations and reanalysis are substantive it is relatively simple to diagnose that there must be an issue in the given reanalysis product as, although imperfect, the uncertainty in the observations can be reasonably bounded. However, many of the differences between candidate reanalysis products and the homogenized reanalyses instead fall into the grey zone whereby the difference is smaller than, or of comparable magnitude to, the potential residual uncertainty in the homogenized series.

The authors could address this point by collecting the substantive family of homogenized temperature station series that have been created over China over the past decade or so and comparing the full family of homogenized series to the full family of reanalyses products. This would serve to substantially strengthen their overall analysis under the assumption that the family of homogenized products and the family of reanalysis products both consist of random draws from the parent distributions of possible homogenized / reanalyzed series. Without undertaking such a

step, although the work may just about be publishable, its utility will be substantively compromised.

Similarly, the observations of the studied covariates (cloudiness, rainfall, radiation etc.) must be uncertain. Again, when differences are substantive inferences can be made without issue. It is when distinctions between the reanalyzed and observed fields are small that interpretation becomes difficult. In such cases the remaining uncertainties in the observations of the covariates limits what inferences can be made.

Response: Thanks for your comments.

Yes, you are right. Single homogenized series is impossibly perfect. In the revised paper, the Student's *t*-test was conducted to difference between reanalysis and homogenized series for considering both uncertainties at the significance level of 0.05. This information was added in the lines **313-315**.

We are keeping cooperating with several Chinese groups, each of which conducts temperature data using different homogeneous methods. These dataset can not be used simultaneously in this study, because they are not of the same time period and identical station, and do not include homogeneous datasets of studied covariates (cloudiness, precipitation frequency, radiation etc.) in this study.

Furthermore, only using the homogeneous time series (not including adjusted time series) at the significance level of 0.05, it can show almost the same results as those from all the time series in the revised paper (see **Fig. 5**).

2)

Comment: Clarity of analysis

In many places the text is hard to follow. This mainly arises through choices as to how to structure the sections and individual paragraphs and this makes it hard as a reader to follow the logical arguments being made by the authors.

The abstract, in particular, is hard to follow as submitted. Efforts at restructuring to make more clearly the arguments the authors wish to put forwards would increase the value of the piece.

The methods section isn't entirely clear and in some places it is questionable whether sufficient detail is given to allow replicability. In particular the set of seven equations is given without sufficiently clear justification and without detail as to whether these are applied gridpoint-wise, smoothed etc.

In the results, the continual listing of regions and reanalyses in different contexts is confusing and hard for a reader to unpick. Greater use of figures and / or tables may serve to improve the messaging aspects here. I find myself trying to connect 12 sets of dots to get a feeling how each reanalysis performs in each aspect in each region and then compare all the joined dots in my head but the problem gets way too big to do so

very quickly. The authors have done a huge amount of analysis but the choice of primarily describing in text without tabular and / or visual ways of summarizing the interconnectedness arguments being made is an impediment to reader understanding.

I find the results, discussion and conclusion sections to be substantively overlapping. These sections would benefit from substantive redrafting and reordering. The results should outline what is found. The discussion should highlight the principal findings and implications. The conclusion should be at most 2-3 paragraphs of key take away messages. Presently the results and discussion feel repetitive and the current conclusions feel to me more like a discussion.

Finally, the text would benefit from substantial input from a native English speaker if available. I am always in two minds over such a comment because I am acutely aware I could write to nothing like the standard in any other language. The authors therefore have my greatest respect for not only undertaking the science but writing it in a second language. But, equally, if the authors wish to have impact they would be served by careful input from a native speaker and it would be remiss of me not to suggest this.

Response: Thanks for your detailed comments. Following your constructive suggestions, we have carefully checked the revised paper and made the logic of Abstract concise and the logic of the revised paper smooth. Especially, we re-edited the Sections Discussion and Conclusions to make them non-overlapping.

We added more details in the **Section Method 2.4** to make it easier to follow: To further investigate the relationship between the spatial distributions of the biases in the trends in T_a and the relevant parameters among the twelve reanalysis products, the weighted total least squares (WTLS) is adopted, **in which the spatial standard deviations and correlations of pairs of variables on $1^{\circ} \times 1^{\circ}$ grid cells were included** (Reed, 1989; York et al., 2004; Golub and Van Loan, 1980; Hyk and Stojek, 2013; Tellinghuisen, 2010).

In the Monte Carlo method, the grid index for the $1^{\circ} \times 1^{\circ}$ grid cells over China, **which ranges from 1 to 691, is generated as a random number**. On this basis, we can sample the spatial pattern in the biases in the trends in T_a , R_s , L_d and precipitation frequency.

We re-plotted **the Fig. 3** to be clearer for reader, especially using different markers for both grouped reanalyses.

Again, following Comment #1 and your suggestions, we have sent out the revised paper for Professional English editing and we have carefully made some language editing in the revised paper.

3)

Comment: Figure suggestions

For the reader it is important that you explicitly define the regions. I would add a new Figure 1 consisting of a map of China in which the different regions are clearly demarcated. The regions are listed in the caption of Figure 1 but there is nothing I can see in Figure 1 which actually denotes this.

Almost all figures use a rainbow colour scale which is inaccessible to those who are colour-blind, which is a not inconsiderable proportion of the population. Numerous colour-blind friendly colour schema are available and consideration should be made as to their use to improve accessibility.

I find many figures hard to understand. The authors are trying to pack a lot of information into these and in many cases because they are postage stamps this is hard to see and interpret. I find Figure 8 particularly difficult and, if I am honest, even after spending 10 minutes trying to understand it suspect that I do not. If you make the reader work this hard they will give up and move on. In general work on making the figures more intuitive and accessible would help enormously.

Response: Thanks for your constructive comments. Please see the region division in **the Fig. 1c** and its corresponding figure caption.

We have made much efforts to try but fail to adopt various colorbars for three variables (***RGB composite***) instead of rainbow colourbars. We also found quite a few literatures used the same rainbow colorbars to plot three variables, e.g., published in *Science* (Nemani et al., 2003) and *Nature* (Seddon et al., 2016).

We re-plotted **the Fig. 3** to be clearer for reader, especially using different markers for both grouped reanalyses. We re-wrote all the relevant figure captions including **the caption of Figure 8** to be concise for easy getting main information.

Reference:

Nemani R R, Keeling C D, Hashimoto H, et al. Climate-driven increases in global terrestrial net primary production from 1982 to 1999[J]. *Science*, 2003, 300(5625): 1560-1563.

Seddon A W R, Macias-Fauria M, Long P R, et al. Sensitivity of global terrestrial ecosystems to climate variability[J]. *Nature*, 2016, 531(7593): 229.

1 **On the Suitability of Current Atmospheric**
2 **Reanalyses for Regional Warming Studies over China**

3
4 Chunlue Zhou¹, Yanyi He¹, Kaicun Wang^{1*}

5 ¹College of Global Change and Earth System Science, Beijing Normal University,
6 Beijing, 100875, China

7
8
9 ***Corresponding Author:** Kaicun Wang, College of Global Change and Earth System
10 Science, Beijing Normal University. Email: kcwang@bnu.edu.cn; Tel.: +86
11 (10)-58803143; Fax: +86 (10)-58800059.

12
13
14
15 Submitted to *Atmospheric Chemistry and Physics*

16 March 13, 2018March 22, 2018

带格式的: 英语(美国)

17 **Abstract**

18 Reanalyses ~~have been~~are widely used because they add value to ~~the~~ routine
19 observations by generating physically ~~or~~and dynamically consistent and spatiotemporally
20 complete atmospheric fields. Existing studies ~~have extensively discussed~~include
21 extensive discussions of the their temporal suitability of reanalyses in global change
22 ~~studies of global change~~. This study ~~moves forward on adds to~~ this existing work
23 by investigating the their suitability of reanalyses in studies of for regional climate
24 change, in which study where land-atmosphere interactions play a ~~more~~
25 comparatively important role. HereIn this study, surface air temperatures~~s~~ (T_a) from 12
26 current reanalysis products ~~were are~~ investigated, focusing on; in particular, the
27 spatial patterns of ~~T_a trend~~trends in T_a are examined, using homogenized
28 measurements of T_a made from 1979 to 2010 at \sim 2200 meteorological stations in
29 China. Results from 1979 to 2010. The results show that \sim 80% of the ~~T_a mean~~
30 ~~differences~~mean differences in T_a between the reanalyses and the in situ
31 observations are can be attributed to the differences in elevation between the stations
32 and the model grid elevation~~model grids~~ differences, denoting good skill in. Thus, the
33 ~~T_a climatology~~climatologies display good skill, and these findings rebutting the
34 ~~previously reported~~previous reports of T_a biases~~biases in T_a~~ . However, the ~~T_a trend~~
35 ~~biases~~biases in the T_a trends in T_a in the reanalyses display spatial divergence~~ed~~diverge
36 spatially (standard deviation=0.15–0.30 °C/decade ~~at using~~ $1^\circ \times 1^\circ$ ~~grid~~grid cells). The
37 simulated ~~T_a trend~~biases~~biases in the trends in T_a correlate well with those of
38 precipitation frequency, surface incident solar radiation (R_s), and atmospheric~~

39 downward longwave radiation (L_d) among the reanalyses ($r=-0.83, 0.80$ and
40 $0.77; p<0.1$) with their spatial patterns of these variables are considered.
Over southern China, the T_a trend biases in the trends in T_a over southern
China (by order of which are on the order of -0.07 °C/decade) are caused by the trend
biases in R_s , biases in the trends in R_s , L_d and the frequency of
precipitation (by order of on the order of 0.10 °C/decade), L_d
(by order of -0.08 °C/decade) and precipitation frequency (by order of and
 -0.06 °C/decade, respectively). Over northern China, the T_a trend biases in the
trends in T_a over northern China (by order of which are on the order of
 -0.12 °C/decade) jointly result from those in L_d and precipitation frequency (the
frequency of precipitation). Therefore, improving the
simulation of precipitation frequency (the frequency of precipitation)
frequency and R_s helps to maximize the regional climate signal component (signal
component corresponding to regional climate). Besides, In addition, incorporating
vegetation dynamics in reanalyses and the use of accurate aerosol information, as in
the Modern-Era Retrospective Analysis for Research and Applications, version
2MERRA-2 (MERRA-2 Modern-Era Retrospective Analysis for Research and
Applications, version 2), would advance result in lead to improvements in the
regional warming modelling (modelling of regional warming). The use of the ensemble
technique (adopted in ERA-20CM, a twentieth-century atmospheric model ensemble ERA-20CM without which does not include the
assimilating assimilation of observations,) significantly narrows the regional warming

61 ~~uncertainties~~associated with regional warming in reanalyses (standard
62 deviation=0.15 °C/decade). Besides, the T_a trend biases show negative spatial
63 correlations (approximately $r=-0.26$, $p=0.00$) with inverted trend in NDVI
64 (Normalized Difference Vegetation Index) implying that incorporating vegetation
65 dynamics can advance regional warming modeling. Inclusion of accurate aerosol
66 information in MERRA-2 (Modern Era Retrospective Analysis for Research and
67 Applications, version 2) helps improve regional climate simulation. ERA-20CM (a
68 twentieth century atmospheric model ensemble without assimilating observations)
69 presents a comparable pattern of the T_a trend biases (standard
70 deviation=0.15 °C/decade) to ERA-Interim and JRA-55 (the Japanese 55-year
71 Reanalysis) that assimilating some T_a observations, which indicates perturbed
72 physical ensemble technique significantly narrows regional warming uncertainties in
73 reanalyses.

74 **1. Introduction**

75 Observations and models are two fundamental approaches ~~to—used in the~~
76 ~~understanding of~~ climate change. ~~The e~~Observations ~~directly provide a direct~~ link
77 ~~with—to the~~ climate system via ~~measuring~~ instruments, ~~whereas—and~~ models ~~has~~
78 ~~provide~~ an indirect link ~~by involving and include~~ information ~~received—derived~~ from
79 measurements~~s~~, prior knowledge and theory.—

80

81 A large number of meteorological observations have been accumulated, ~~including~~.
82 ~~These measurements, which are derived from a variety of sources, such as surface~~
83 ~~stations, ships, buoys, radiosondes, airplanes and satellites, record quantities that~~
84 ~~include~~ near-surface and upper-air temperatures~~s~~, humidity, wind and pressure ~~from a~~
85 ~~variety of sources surface stations, ships, buoys, radiosondes, airplanes and satellites.~~
86 They constitute a major source of atmospheric information through the depth of ~~the~~
87 troposphere but suffer from incomplete spatiotemporal coverage and ~~observed~~
88 ~~errorobservation errors~~, including systematic, random and ~~representative~~
89 ~~representation~~ errors. Recent satellite-based observations have much better coverage
90 ~~but; however, they~~ suffer from other ~~notable~~ limitations~~s~~, including ~~notably~~ temporal
91 inhomogeneit~~iesy~~ (e.g., satellite drift) and retrieval errors~~s~~ (Bengtsson et al., 2007).
92 These ~~space time spatiotemporally~~ varying gaps restrict the ~~effective application of~~
93 observations alone ~~to be effectively applied~~ in climate research.

94 To fill in the gaps in ~~the~~ observations, ~~a~~models ~~is—are~~ needed. ~~The Such~~ models
95 ~~can can~~ be very simple, ~~e.g.: examples of simple models include~~ linear interpolation

96 or geo-statistical approaches that are based on the spatial and temporal autocorrelation
97 of the observations. However, these models lack the necessary dynamical or physical
98 mechanisms. With Given the steady progress in-the of numerical weather prediction
99 (NWP) models in echaracteringcharacterizing the global atmospheric circulation in
100 the early 1980s (Bauer et al., 2015), an originalthe first generation of ‘reanalyses’
101 was was achieve produced by combining observations and dynamic models to provide
102 the first global atmospheric datasets available for use in scientific research (Bengtsson
103 et al., 1982a, b).

104 After realizing the great value of this kind of reanalysis for in atmospheric
105 research, a step forward was was taken with the suggestion made by Bengtsson and
106 Shukla (1988) and Trenberth and Olson (1988) that most meteorological observations
107 should be optimally assimilated under a fixed dynamical system over a period of time
108 long enough to be useful for climate studies. In this way, available observations are
109 ingested by advanced data-assimilation techniques to provide a continuous initial
110 state for an the NWP model to produce the next short-term forecast, t. This procedure
111 thus generating generates physically consistent and spatiotemporally complete
112 three-dimensional atmospheric fields that are updated in light of observations.

113 Under thisTaking this suggestion as a guide, and given the improvements that
114 have been made since the mid-1990s in the integrity of the observations, the models
115 and the assimilation methods used, successive generations of atmospheric reanalyses
116 established by several institutes have improvements improved in quality with better
117 observation integrity, better models and better assimilation methods since the

118 ~~mid-1990s~~. These reanalyses include the first two generations of global reanalyses
119 ~~from produced by~~ the National Centers for Environmental Prediction-~~f~~-NCEP-R1
120 (Kalnay et al., 1996) and NCEP-R2 (Kanamitsu et al., 2002)~~f~~ and the reanalyses
121 ~~produced by~~; the European Centre for Medium-Range Weather Forecasts (ECMWF)-~~f~~
122 ERA-15 (Gibson et al., 1997), ERA-40 (Uppala et al., 2005)~~f~~ and ERA-Interim (Dee
123 et al., 2011b)~~f~~, the Japanese Meteorological Agency-~~f~~-JRA-25 (Onogi et al., 2007)
124 and JRA-55 (Kobayashi et al., 2015)~~f~~ and the National Aeronautics and Space
125 Administration-~~f~~, the Modern-Era Retrospective Analysis for Research and
126 Applications (MERRA) (Rienecker et al., 2011) and its updated version, MERRA-2
127 (Reichle et al., 2017)~~f~~.

128 These reanalyses produce global gridded datasets that cover multiple time
129 -scale~~sd, global gridded datasets including and include~~ a large variety of atmospheric~~ice,~~
130 ~~sea oceanic~~ and land surface parameters, many of which are not easily or routinely
131 observed but ~~are~~ dynamically constrained by ~~a great number~~large numbers of ~~multiple~~
132 ~~sourced observations~~observations from multiple sources assimilated ~~under using~~
133 fixed NWP models~~s~~. During the data assimilation, prior information ~~about on~~
134 uncertainties in the observations and models~~s~~ are used ~~for to perform~~ quality checks, to
135 derive bias adjustments and to assign~~their~~ proportional weights. Therefore, such
136 reanalyses add value to the instrumental record ~~in the aspects of through their~~
137 inclusion of bias adjustments, their broadened spatiotemporal coverage and their
138 increased dynamical ~~integrity~~integrity or consistency.

139 Previous studies have revealed that such reanalyses have contributed significantly

140 to a more detailed and comprehensive understanding of the dynamics of the Earth's
141 atmosphere (Dee et al., 2011b; Kalnay et al., 1996; Nguyen et al., 2013; Kidston et
142 al., 2010; Simmonds and Keay, 2000; Simmons et al., 2010; Mitas and Clement,
143 2006). Extensive assessment studies have reported that most reanalyses have display a
144 certain level of performance in terms of their absolute values (Betts et al., 1996; Zhou
145 and Wang, 2016a; Betts et al., 1998), interannual variability (Lin et al., 2014;
146 Lindsay et al., 2014; Zhou and Wang, 2017a, 2016d; Wang and Zeng, 2012),
147 distributions (Gervais et al., 2014; Heng et al., 2014; Mao et al., 2010) and
148 relationship of inter-s among variables (Niznik and Lintner, 2013; Cash et al., 2015;
149 Zhou et al., 2017; Zhou and Wang, 2016a; Betts, 2004) over regions worldwide.
150 However, these aspects of reanalyses still contain~~here are still~~ certain errors in these
151 aspects so as to that restrict the~~is~~ general use of reanalyses, especially for in climate
152 applications.

153 These errors emerging in~~displayed by~~ reanalysis products can be summarized
154 into~~arise from~~ three sources: observation error, model error and assimilation error
155 (Thorne and Vose, 2010; Parker, 2016; Lahoz and Schneider, 2014; Dee et al., 2014;
156 Zhou et al., 2017). Specially, Specifically, the—observation error incorporates
157 systematic and /random errors in instruments and its—their replacements, errors in data
158 reprocessing and representative error~~representation error in, which arises due to the~~
159 spatiotemporal incompleteness of observations (Dee and Uppala, 2009; Desroziers et
160 al., 2005);~~the m.~~ Model error mainly refers mainly to the inadequate representation of
161 physical processes in the NWP models (Peña and Toth, 2014; Bengtsson et al., 2007),

162 ~~e.g., such as the~~ lack of time-varying ~~setting of~~ surface conditions~~+~~_{such as vegetation}
163 growth (Zhou and Wang, 2016a; Trigo et al., 2015) and incomplete
164 cloud-precipitation-radiation parameterizations (Fujiwara et al., 2017; Dolinar et al.,
165 2016); ~~the a.~~ Assimilation error ~~involves describes mapping~~ errors ~~that arise in the~~
166 ~~mapping~~ of ~~the~~ model space to ~~the~~ observation space and errors~~s~~ in the topolog~~iesy~~ of
167 ~~the~~ cost functions (Dee, 2005; Dee and Da Silva, 1998; Lahoz and Schneider, 2014;
168 Parker, 2016).

169 These reanalyses ~~mentioned~~ above consist of the true climate signal and ~~the some~~
170 nonlinear interactions among ~~the~~ observation error, ~~the~~ model error, and ~~the~~
171 assimilation error ~~that arise~~ during the assimilation process. These time-varying errors
172 can ~~thus~~ introduce ~~a fictitious spurious~~ trends~~s~~ without being eliminated by ~~the~~ data
173 assimilation system~~s~~. Many spurious variations in ~~the~~ climate signals ~~have were been~~
174 ~~also also~~ identified in the ~~early early~~-generation reanalyses (Bengtsson et al., 2004;
175 Andersson et al., 2005; Chen et al., 2008; Zhou and Wang, 2016d, 2017a; Zhou et
176 al., 2017; Schoeberl et al., 2012; Xu and Powell, 2011; Hines et al., 2000; Cornes
177 and Jones, 2013). Therefore, ~~the reanalyseis produced under using the guide of~~ the
178 existing reanalysis strategy may not accurately capture ~~the~~ climate trends (Trenberth
179 et al., 2008), even though ~~they may contain having a~~ relatively accurate estimates~~s~~ of
180 synoptic or interannual variations ~~of in~~ the Earth's atmosphere.

181 An emerging requirement for climate applications of reanalysis data is the
182 accurate representation of decadal variability, further increasing the confidence in the
183 estimation~~one~~ of climate trends. This kind of climate reanalysis is required to be ~~to great~~

184 extent free, to a great extent, from other spurious non-climatic signals introduced by
185 changing observations, imperfect model imperfections and assimilation error,
186 i.e., to keep the time consistency; that is, they must maintain temporal consistency.
187 Therefore, the extent to which the estimate of climate trends by climate can be
188 assessed using reanalysis is can be realized attracts much attention and sparks
189 heated debates (Thorne and Vose, 2010; Dee et al., 2011a; Dee et al., 2014;
190 Bengtsson et al., 2007).

191 With Given the great progress that has been made in climate forecasting models
192 (which provide more accurate representations of climate change and variability) and
193 coupled data assimilation, a lot of many efforts have been made by several institutes
194 to build the consistent climate reanalysis under the climate strategy that using the
195 strategy of assimilating a relatively few small number of but high-quality long-term
196 observational datasets. The climate reanalyses of this new generation of climate
197 reanalyses extend back to the late nineteenth century and are include the Climate
198 Forecast System Reanalysis (CFSR), which is produced by the National Centers
199 for Environmental Prediction CFSR (Saha et al., 2010); NOAA 20CRv2c, which is
200 produced by the University of Colorado's Cooperative Institute for Research in
201 Environmental Sciences (CIRES) together in cooperation with the National Oceanic
202 and Atmospheric Agency (NOAA) NOAA 20CRv2e (Compo et al., 2011); and
203 ERA-20C (Poli et al., 2016), ERA-20CM (Hersbach et al., 2015) and CERA-20C
204 (Laloyaux et al., 2016), which are produced by the ECMWF ERA-20C (Poli et al.,
205 2016), ERA-20CM (Hersbach et al., 2015) and CERA-20C (Laloyaux et al., 2016).

206 Compo et al. (2013) suggested that the NOAA 20CRv2c reanalysis can reproduce the
207 trend in global mean surface air temperatures. In addition, the uncertainties estimated
208 from multiple ensembles are provided to increase the confidence of the climate trends
209 (Thorne and Vose, 2010; Dee et al., 2014).

210 From ~~the~~ NWP-like reanalyse~~s~~ to climate reanalyse~~s~~, existing researches~~studies~~
211 ~~mainly focus on~~focus mainly on comparing the differences in temporal variability
212 between the reanalyses and observations, using some statistical metrics, e.g., the mean
213 values, standard deviations, interannual correlations, probability density functions and
214 trends of surface air temperature over regions worldwide. These evaluations actually
215 provide ~~an~~-insight into the temporal evolution of the Earth's atmosphere. However, ~~it~~
216 ~~lacksthey lack~~ the performance evaluations of used in reanalyse~~s~~ in representing the
217 spatial patterns of these statistics associated with the role of the coupled
218 land-atmosphere and dynamical processes of the climate system. Moreover, the
219 assessment of these spatial patterns provides a direct ~~way to~~means of examin~~ing~~ the
220 most distinguished prominent advantage of reanalyse~~s~~~~is that over the~~ geo-statistical
221 interpolation~~does not have, and thereby; thus,~~ the ~~assessment of the~~ spatial patterns
222 ~~remains to be~~require comprehensively investigat~~ioned~~.

223 ~~Using This study employs the highly dense~~high-density station-based datasets of
224 quantities including surface air temperatures (T_a), the surface incident solar radiation
225 (R_s), the surface downward longwave radiation (L_d), and precipitation measured from
226 ~~1979 to 2010~~ at ~2200 meteorological stations within China from 1979 to 2010 over
227 ~~China, this study provides. It provides~~ a quantitative examination of the simulated

228 patterns of ~~T_a-variations~~variations in T_a from in both the the-NWP-like ~~and to~~ climate
229 reanalyses, ~~including and considers the~~ climatology, ~~the~~ interannual variability, ~~the~~
230 mutual relationships~~s-between among~~ relevant quantities, ~~the~~ long-term trends and
231 their controlling factors. The results ~~identified indicate the~~ strengths and weaknesses
232 of the current reanalyses ~~when applied in~~ regional climate change studies and
233 provide possible ways to improve ~~these~~ reanalyses in the near future.

234

235 **2. Data and Methods**

236 **2.1 Observation Data**Observational Datasets

237 The latest comprehensive daily dataset (~~which contains~~ averages~~s~~ at 0, 6, 12, ~~and~~
238 18 UTC) ~~of quantities including that include~~ T_a, precipitation, sunshine duration,
239 relative humidity, water vapor pressure, surface pressure and ~~the~~ cloud fraction from
240 approximately 2400 meteorological stations in China from 1961 to 2014, ~~out~~ of which
241 only approximately 194 ~~participate in~~ global exchanges~~s~~, ~~wasis~~ obtained from the
242 China Meteorological Administration (CMA~~s~~, <http://data.cma.cn/data>). Approximately
243 2200 stations with complete and homogeneous data ~~were are~~ selected ~~for use~~ in this
244 study (Wang and Feng, 2013~~s~~; Wang, 2008~~s~~; Wang et al., 2007). ~~The h~~Hight density of
245 meteorological stations in China ~~is beneficial to promotes the representation of and~~
246 ~~assess the simulated skill of~~ regional patterns in surface warming by reanalyse~~s~~ is and
247 the assessment of the skill of simulations.

248 ~~The R_s values~~ based on the revised Ångström-Prescott equation (Wang et al.,
249 2015~~s~~; Yang et al., 2006~~s~~; Wang, 2014) ~~was are~~ used in this study. The derived R_s ~~has~~

带格式的：缩进：首行缩进： 0 字符

250 ~~eonsidered~~values consider the effects of Rayleigh scattering, water vapor absorption
251 and ozone absorption (Wang et al., 2015; Yang et al., 2006) and can accurately reflect
252 the ~~impact effects~~ of aerosols and clouds on R_s over China (Wang et al., 2012; Tang
253 et al., 2011). Several intensive studies have reported that the derived R_s values can
254 accurately depict the interannual, decadal and long-term ~~varianees of variations in~~ R_s
255 (Wang et al., 2015; Wang, 2014; Wang et al., 2012).

256

257 ~~The~~ L_d is typically estimated by first determining the clear-sky radiation and atmospheric emissivity (Brunt, 1932; Choi et al., 2008; Bilbao and De Miguel, 2007),
258 and then correcting for ~~the~~ cloud fraction (Wang and Liang, 2009; Wang and Dickinson, 2013). The derived L_d values can directly reflect ~~the~~ greenhouse effect of ~~atmosphere water~~atmospheric water vapor and clouds. Additionally, a precipitation event ~~was is~~ defined as ~~daily one day with~~ precipitation of at least 0.1 mm-daily in this study, which ~~was has been~~ shown ~~as to provide~~ a good ~~indicator in reflecting~~indication of the effects of precipitation ~~impact~~ on ~~the~~ interannual variability and trends ~~of in~~ T_a (Zhou et al., 2017). ~~In all, Taken together,~~ the derived R_s and L_d values are able to physically quantify ~~the effects of~~ solar radiative ~~effeeton~~ and ~~the~~ greenhouse effect on surface warming. ~~Precipitation frequency~~The frequency of precipitation ~~Precipitation frequency~~ can regulate the partitioning of available energy into latent and sensible heat fluxes, and ~~then thus~~ modulates ~~s~~ the ~~variance of variations in~~ T_a (Zhou et al., 2017; Zhou and Wang, 2017a).

271 **2.2 Reanalysis Products**

带格式的：缩进：首行缩进：0 字符

272 All theAll of the major global atmospheric reanalysis products were-are included
273 in this study (Table 1). The reanalyses were-are summarized below from-in terms of
274 three aspects, i.e., the observations assimilated— and the forecast model and
275 assimilated methodassimilation method used. The NWP-like reanalyses assimilate~~d~~
276 many of multi-soured conventional and satellite datasets from multiple sources
277 (Table 1), whose spatiotemporal errors vary with time, to characterize the basic
278 upper-air atmospheric fields; the spatiotemporal errors of these datasets vary with
279 time. In particular, the ERA-Interim and JRA-55 reanalyses incorporate some
280 observations of T_{a2} and the MERRA2 reanalysis includes aerosol optical depth
281 estimates from satellite retrievals and model simulations based on emission
282 inventories, whereas most of the other reanalyses use the climatological aerosols
283 (Table 1). To derive long term consistent long-term climate signals, the new strategy
284 that adopted by climate reanalyses adept is to involves the assimilation of a small
285 number of few but relatively effective observationsobserved variables, e.g., surface
286 pressure (Table 1). Except for no its lack of the assimilation of surface pressure,
287 ERA-20CM has employs the same forecast model and external forcings as ERA-20C
288 (Table 1), so; thus, the inclusion of ERA-20CM here-in this study will provide an
289 insight into the suitability of current atmospheric reanalyses in regional warming
290 studiesstudies of regional warming. The reanalyses adopt different sea surface
291 temperatures (SSTs) and sea ice concentrations for different time periods, maybe
292 leadingwhich may lead to temporal discontinuities in the climate signals derived from
293 the reanalyses (Table 1). To address this issue, the boundary conditions in the CFSR is

294 ~~are generated by~~^{derived from} its coupled ocean-sea ice models instead of ~~the~~
295 observations (Table 1). ~~The~~-CFSR, NOAA 20CRv2c and NOAA 20CRv2 use ~~the~~
296 monthly greenhouse gases (GHGs) with annual means near ~~the~~^{those used in} CMIP5~~–~~
297 ~~On the other hand, in the~~ ERA-Interim ~~has a slower increase of,~~ the GHGs ~~increase~~
298 ~~more slowly than in the~~ CMIP5 after 2000~~–~~. Finally, ~~the~~ NCEP-R1 and NCEP-R2
299 adopt constant global mean ~~concentrations~~ of ~~the~~ GHGs (Table 1).

300 The forecast model is a fundamental component of ~~a~~ reanalysis~~s~~ that provides the
301 background fields to the assimilation system. ~~The~~ Different reanalyses ~~in an~~^{produced}
302 ~~by a single~~ institute generally use similar ~~but updated~~ physical parameterizations~~:~~
303 ~~however, updated versions of these parameterizations~~ and higher spatial resolutions
304 ~~are used~~ in ~~the~~ newer generations ~~of these realizations~~ (Table 1). The assimilation
305 methods adopted by the current reanalyses incorporate variational methods (3D-Var
306 and 4D-Var) and the ~~Ensemble ensemble~~ Kalman ~~f~~Filter (EnKF) ~~approach~~ (Table 1).
307

308 The 2-m T_a in NCEP-1, NCEP-2, MERRA, MERRA-2, ERA-20C, ERA-20CM,
309 CERA-20C, NOAA 20CRv2c, NOAA 20CRv2 and CFSR are model-derived fields~~as~~
310 ~~a that are~~ functions of ~~the~~ surface skin temperature ~~and the,~~ ~~the~~ temperature at the
311 lowest model level, ~~the~~ vertical stability and ~~the~~ surface roughness ~~that were, which~~
312 ~~are primarily~~ constrained ~~primarily~~ by observations of upper~~–~~air variables and ~~the~~
313 surface pressure (Kanamitsu et al., 2002~~;~~; Rienecker et al., 2011~~;~~; Reichle et al., 2017~~;~~
314 Poli et al., 2016~~;~~; Hersbach et al., 2015~~;~~; Laloyaux et al., 2016~~;~~; Compo et al., 2011~~;~~
315 Saha et al., 2010). Yet, ~~However,~~ the T_a ~~values~~ in ERA-Interim and JRA-55 ~~are~~

316 ~~post-processing products by result from more post-processing performed products~~
317 ~~by using~~ a relatively simple ~~analysis interpolation analysis~~ scheme between the lowest
318 model level and the surface ~~and are, analyzed analysed with using some~~ ground-based
319 observations of T_a , ~~with the help of combined with the help of~~ Monin-Obukhov
320 similarity profiles consistent with the model's parameterization of the surface layer
321 (Dee et al., 2011b; Kobayashi et al., 2015). Additionally, radiation calculations are
322 diagnostically determined from the prognostic cloud condensate microphysics
323 parameterization, and ~~the~~ cloud macrophysics ~~parameterization~~ assumes a
324 maximum-random cloud overlapping ~~scene scheme~~ (Saha et al., 2010; Dolinar et al.,
325 2016).

326 **2.3 Method Used to Homogenize the Observed Time Series**

327 ~~The p~~roblems related to the observational infrastructure (e.g., instrument ~~aging~~
328 ~~ageing~~ and changes in observing practices) and station relocations can also lead to
329 false ~~time temporal~~ heterogeneity in time series. Therefore, ~~it's it is~~ necessary to
330 diminish the impact of data homogenization on the trends in the observed variables
331 during the study period ~~of~~ 1979-2010.

332 We used the RHtestsV4 software package (Wang and Feng, 2013) to detect and
333 homogenize the breakpoints in the monthly time series. The package ~~involves~~
334 ~~includes~~ two algorithms: ~~. Specifically,~~ the PMFred algorithm is based on the
335 penalized maximal F -test (*PMF*) without a reference series (Wang, 2008), and the
336 PMTred algorithm is based on the penalized maximal t -test (*PMT*) with a reference
337 series (Wang et al., 2007).-

338
339 In this study, we first used the PMFred algorithm to find identify potential
340 reference series at the 95% significant levelsignificance level. Then, weWe then
341 reconstructed homogenous series for each inhomogeneous series by using the
342 following steps: 1) horizontal and vertical distances from the inhomogeneous station
343 of less than 1100km km horizontally distant from the inhomogeneous station and
344 5000m m vertical height difference, respectively, are specified; 2) correlation
345 coefficientsover 0.9 of between the first-order difference in the homogeneous series
346 with that in the inhomogeneous one exceeding 0.9 are required; and 3) the first ten
347 homogeneous series was are inverse distance weightedly averagedaveraged using
348 inverse distance weighting as to produce a reference series for the inhomogeneous
349 one station. Finally, we applied apply the PMTred algorithm to test all the all of the
350 inhomogeneous series with using the nearby reference series nearby. Several intensive
351 researches studies were have been conducted to show a that indicate good performance
352 of the PMTred algorithm displays good performance – in detecting change points of
353 in inhomogeneous series (Venema et al., 2012; Wang et al., 2007).

354 If the a breakpoint is found to be statistically significant, the quantile-matching
355 (QM) adjustment in RHtestsV4 is recommended for making adjustments to the time
356 series (Wang et al., 2010; Wang and Feng, 2013), based on; in such cases, the longest
357 available segment from 1979 to 2010 is used as the base segment. The QM
358 adjustment aims to match the empirical distributions from all of the detrended
359 segments with that of the specific base segment (Wang et al., 2010). In addition, we

360 replicated the procedures above for the sparingly distributed~~sparse~~ stations over
361 western China ~~and Tibetan~~and the Tibetan Plateau. ~~Recently, t~~The PMTred algorithm
362 ~~with and~~ the QM adjustment ~~was have recently been successfully~~ used successfully to
363 homogenize climatic time series (Aarnes et al., 2015; Tsidu, 2012; Dai et al., 2011;
364 Siswanto et al., 2015; Wang and Wang, 2016; Zhou et al., 2017).

365 As such, the significant breakpoints ~~over 1092 out of 2193 (49.8%) stations~~
366 ~~were are~~ detected and adjusted at a confidence level of 95% at 1092 of the 2193
367 (49.8%) stations for the T_a time series; 1079 ~~out of~~of the 2193 (49.2%) stations for
368 the R_s time series; 64 ~~out of~~of the 2193 (2.9%) stations for precipitation frequency~~the~~
369 ~~frequency of precipitation~~precipitation frequency time series; 971 ~~out of~~of the 2193
370 (44.2%) stations for the L_d time series; 944 ~~out of~~of the 2193 (43.0%) stations for the
371 water vapor pressure time series; and 956 ~~out of~~of the 2193 (43.6%) stations for the
372 cloud fraction time series.

373 **2.4 Trend Calculations, Partial Linear Regression, and Total Least Squares**

374 The bias, ~~root-mean-square-root mean squared~~ error (RMSE), standard deviation
375 and correlation coefficient (r) ~~were are~~ used to assess the absolute value of T_a . The
376 ~~trends in T_a~~ Trends in T_a and the relevant variables ~~were are~~ calculated using the
377 ordinary least squares method (OLS) and the two-tailed Student's t -test. To determine
378 whether the reanalyses contain trend bias~~biases in these trends exists in reanalysis~~, the
379 two-tailed Student's t -test ~~was is~~ also applied to the differences ~~of in the~~ time series
380 between the reanalyse~~is~~ and the homogeneous observations.

381 The partial least squares approach ~~was is~~ used to investigate the net relationship ~~of~~

382 ~~between the~~ detrended T_a ~~values with~~~~and the~~ relevant variables (R_s , L_d and
 383 ~~precipitation frequency~~~~the frequency of precipitation~~~~precipitation frequency~~) after
 384 statistically excluding the confounding effects among ~~the~~ relevant variables (Zhou et
 385 al., 2017). To evaluate ~~the~~ potential ~~eolinear~~~~collinear~~ity of independent variables in
 386 the ~~regress model~~~~regression model~~, the variance inflation factor (VIF) ~~was is~~
 387 calculated. The VIFs for R_s , ~~precipitation frequency~~~~the frequency of~~
 388 ~~precipitation~~~~precipitation frequency~~ and L_d ~~were are~~ less than 4, e.g., ~~Specifically, the~~
 389 ~~VIFs of for China of 2.19 for China, is~~ much less than the threshold of 10, above
 390 which the collinearity of ~~the regress model~~~~regression models~~ is bound to adversely
 391 affect the regression results (Ryan, 2008).

392 The Pearson correlation ~~analysis coefficient was is~~ used to reveal the spatial
 393 relationship ~~of T~~~~between T_a with relevant variables~~~~and the relevant variables~~. To
 394 further investigate the relationship ~~of~~~~between the~~ spatial distributions of the T_a trend
 395 ~~biases~~~~biases in the trends in T_a with and~~ the relevant parameters among the twelve
 396 reanalysis products, the weighted total least square~~s~~ (WTLS) ~~metric was is~~ adopted, in
 397 which the spatial standard deviations and correlations of ~~both pairs of~~ variables ~~at on~~
 398 $1^\circ \times 1^\circ$ ~~grids~~~~grid cells~~ ~~were are~~ included (Reed, 1989; York et al., 2004; Golub and
 399 Van Loan, 1980; Hyk and Stojek, 2013; Tellinghuisen, 2010):

$$\omega(x_i) = 1/\hat{\sigma}_{x_i}^2 \quad (1)$$

$$\omega(y_i) = 1/\hat{\sigma}_{y_i}^2 \quad (2)$$

$$W_i = \frac{\omega(x_i) \cdot \omega(y_i)}{\omega(x_i) + b^2 \omega(y_i) - 2b \cdot r_i \sqrt{\omega(x_i) \cdot \omega(y_i)}} \quad (3)$$

带格式的：字体：倾斜

403
$$U_i = x_i - \sum_i^n (W_i \cdot x_i) / \sum_i^n (W_i)$$
 (4)

404
$$V_i = y_i - \sum_i^n (W_i \cdot y_i) / \sum_i^n (W_i)$$
 (5)

405
$$\beta_i = W_i \left[\frac{U_i}{\omega(y_i)} + \frac{b \cdot V_i}{\omega(x_i)} - (b \cdot U_i + V_i) \frac{r_i}{\sqrt{\omega(x_i) \cdot \omega(y_i)}} \right]$$
 (6)

406
$$b = \frac{\sum_{i=1}^n W_i \cdot \beta_i \cdot V_i}{\sum_{i=1}^n W_i \cdot \beta_i \cdot U_i}$$
 (7)

407 where x_i and y_i are the median trends in x and y ~~variable (including e.g., T_a and, R_s and so-on)~~ at for the i^{th} reanalysis product~~s~~, $\hat{\sigma}_{x_i}$, $\hat{\sigma}_{y_i}$ and r_i are the spatial standard deviations and correlations of the trends in x and y ~~variables at for the~~ i^{th} reanalysis product~~s~~, β_i is the least-squares-adjusted value~~and~~, W_i is the weight of the residual error~~s~~ and b is the slope estimated by iterative method~~s~~ with a relative tolerance of 10^{-16} .

413 The Monte Carlo method with 10000 experiments ~~wasis~~ applied to estimate the
 414 90% confidence intervals of the slope b . In the Monte Carlo method, the grid index
 415 ~~for the $1^\circ \times 1^\circ$ grid cells over China is generated as random number, i.e., the, which~~
 416 ~~ranges from 1 to -691, grid index for the $1^\circ \times 1^\circ$ grids over China is generated as a~~
 417 ~~random number, based on which we could. On this basis, we can~~ sample the spatial
 418 pattern in ~~the trends biases inbiases in the trends in~~ T_a , R_s , L_d and ~~precipitation~~
 419 ~~frequency the frequency of precipitation~~ precipitation frequency. Then, we
 420 ~~eaculatedWe then calculate~~ the median trends and their spatial standard deviations
 421 and correlations for each experiment~~s~~ used in the WTLS.

422

423 **3. Results**

424 **3.1 Dependency of Surface Air Temperature DifferencesBiases on Elevation**

425 **DifferencesDependency of Surface Air Temperature Bias**

426 Fig. 1 illustrates the differences in T_a from the NWP-like reanalysisis and climate
427 reanalysisis relative to the homogenized station-based observations over China during
428 the period 19period of 1979-2010. If directly compareWhen the T_a values measured at
429 the stations are compared directly with those atin the corresponding model gridsgrid
430 cellsand stations, the results indicate that the reanalysis products exhibit an
431 underestimated underestimate T_a over most of the regions of in China (by -0.28 °C to
432 -2.56 °C in China), especially. These discrepancies are especially pronounced over the
433 Tibetan Plateau (-2.75 °C to -7.00 °C) and Middle China, where the underestimation
434 ranges from -2.75 °C to -7.00 °C and from (-1.19 °C to -2.91 °C, respectively) (Fig. 1
435 and Table 2). A homogeneous adjustment of 0.033 °C from the raw T_a observations
436 is insufficient to cancel the underestimation of T_a by the reanalyses (Fig. 1 and Table
437 2). The sSimilar results of biases in T_a within various regions worldwide bias have
438 been widely reported by previous studiesover regions worldwide (Mao et al., 2010;:
439 Pitman and Perkins, 2009;: Reuten et al., 2011;: Wang and Zeng, 2012;: Zhou et al.,
440 2017;: Zhou and Wang, 2016a).

441 However, we found that the spatial patterns in the differences in T_a are well
442 correlated with the elevation differences between models and stations, as reflected by
443 with correlation coefficients (r) of 0.85 to 0.94 (Figs. 2 and S1), which is in. These

444 results are in accordance with the reports from NCEP-R1, NCEP-R2 and ERA-40
445 (You et al., 2010; Ma et al., 2008; Zhao et al., 2008). The elevation differences
446 (ΔH) between the stations and the model grids consists of the
447 filtering error in the elevations used in the spectral model-elevations (Δf) and
448 differences in the site-to-grid elevations (Δs) due to the complexity of the orographic
449 topography. We further quantified their relative contributions of these
450 factors to the T_a differences. The elevation differences can explain approximately 80%
451 of the T_a differences, among which, approximately 74% is from produced by the
452 site-to-grid elevation differences, and approximately 6% is from produced by the
453 filtering error in the elevations used in the spectral model-elevations (Fig. 2).

454 One can find that the regression coefficient of the
455 differences in T_a is approximately $6\text{ }^{\circ}\text{C}/1\text{ km}$, near which is similar to the lapse
456 rate at the surface (Fig. 2). The Lapse rate values over that exceed $6\text{ }^{\circ}\text{C}/1\text{ km}$ can
457 be seen over Tibetan over the Tibetan Plateau (shown as red dots in Fig. 2; in red dots).
458 This result is very consistent with the reported lapse rates over China (Li et al., 2015;
459 Fang and Yoda, 1988). In addition, the decreasing rate of decrease in the model
460 filtering error is approximately $4\text{ }^{\circ}\text{C}/1\text{ km}$ among the twelve reanalyses twelve
461 reanalyses (Fig. 2). These results above have an important implications for a good the
462 skill in the simulation of the simulated T_a climatology climatologies of T_a in the
463 twelve reanalyses over China.

464 3.2 Comparison of Regional-scale Surface Air Temperature Series

465 Fig. 3 shows the Taylor diagrams of annual T_a anomalies from the observations

466 and reanalyses over China and its seven subregions. We ~~found~~find that the
467 correlations ~~of annual T_a anomalies~~ between the annual T_a anomalies in the ~~twelve~~
468 ~~reanalysis~~twelve ~~product~~reanalysis products and the observations are ~~pretty~~
469 ~~reasonably~~ strong ~~with~~, as reflected by a median r of 0.95 (Fig. 3), despite ~~of the~~
470 relatively weak correlations ~~over Tibetan~~over the Tibetan Plateau ~~for~~ associated with
471 NCEP-R2 ($r=0.24$) and CFSR ($r=0.53$). The simulated time series of T_a anomalies
472 over eastern China are depicted most accurately by the reanalyses (Fig. 3c-g).

473 Overall, the NWP-like reanalyses (denoted by numbers 3-7) ~~have adisplay~~ better
474 skill than ~~the~~ climate reanalyses (denoted by numbers 8-14) ~~at this aspectin this~~
475 ~~regard~~ (Fig. 3). ~~The~~ ERA-Interim and JRA-55 ~~has display~~ the best performance in the
476 simulated time series of T_a anomalies over China ($r=1.00$, RMSE=0.05 °C) and the
477 seven regions ($r=0.98$, RMSE=0.1 °C) (Fig. 3), ~~may be perhaps~~ due to ~~their analysis~~the
478 incorporation~~their analysis~~ of surface air temperature observations in ERA-Interim
479 and JRA-55 (Table 1).

480 Compared ~~withing~~ the T_a values from MERRA2 ~~to and~~ MERRA shows that; we
481 ~~found that the~~ MERRA2 ~~has and displays~~ improved performance over ~~n~~Northern China
482 ~~by an, as reflected by an increasing increase in the~~ correlation coefficient of 0.1 and a
483 ~~reduction in the~~ RMSE of 0.1 °C (Fig. 3), ~~maybe. This result may occur~~ because ~~the~~
484 MERRA2 includes ~~the~~ time-varying aerosol loadings (Balsamo et al., 2015; Reichle
485 et al., 2011). However, ~~this circumstance~~the incorporation of this information does not
486 improve the results over Southeast China (Fig. 33hh).

487 ~~The~~ CERA-20C ~~has a~~ displays better performance than ERA-20C and

488 ERA-20CM, ~~may be perhaps~~ related to ~~an the~~ inclusion of coupled climate forecast
489 models~~s~~ and data assimilation, as well as the assimilation of surface pressure
490 assimilated data in CERA-20C (Fig. 3 and Table 1). ~~The~~ NOAA 20CRv2c and NOAA
491 20CRv2 ~~have adisplay~~ moderate performance in this ~~aspeet regard~~ ($r=0.8$,
492 RMSE=0.3–~~€3~~ °C) (Fig. 3), and the former reanalysis has displays no improvement
493 in performance, despite ~~of the its~~ use of new boundary conditions~~s~~ (Compo et al.,
494 2011).

495 3.3 Key Factors Regulating Regional Temperature Change

496 This section discusses key factors ~~controlling that control~~ regional temperature
497 change from ~~a the~~ perspective of energy balance and its partitioning. The R_s heats the
498 surface, and the portion of this radiation that becomes the sensible heat flux-surface
499 heats the air near the surface by partitioning into sensible heat flux (Zhou and Wang,
500 2016a; Wang and Dickinson, 2013; Zhou and Wang, 2016b). ~~The pP~~art of the energy
501 absorbed by the surface is released back to ~~s~~pace as outgoing longwave radiation,
502 ~~some of which; some of this radiation~~ is reflected by clouds and is influenced by
503 atmospheric water ~~vapor~~vapor, further warming the near-surface air (Wang and
504 Dickinson, 2013). This process is known as the greenhouse effect (~~quantified by the~~
505 L_d on T_a and is quantified by L_d). Existing studies have suggested that ~~precipitation~~
506 ~~frequency~~the frequency of precipitationprecipitation frequency is a better factor in
507 quantifyingbetter represents the interannual variability ofvariability in soil moisture
508 ever in China than the precipitation amount (Wu et al., 2012; Piao et al., 2009; Zhou
509 et al., 2017; Zhou and Wang, 2017a), and then; in turn, soil moisture changes affects

510 vegetation growth and ~~surface characteristics~~ drives changes in surface
511 ~~characteristics~~ (e.g., e.g., surface albedo and roughness). These changes ~~would~~ alter
512 the partitioning of available energy ~~for regulating and thus regulate the~~ changes in T_a .

513

514 Figs. 4 illustrates the partial relationships between the annual anomalies in T_a and
515 R_s -anomalies, the precipitation frequencyfrequency of precipitation frequency and L_d .
516 Results. The results show that T_a has is consistently positively correlations
517 correlated with R_s (except over the Tibetan Plateau) and L_d , but has; however, it is
518 consistently negatively correlations correlated with precipitation frequency the
519 frequency of precipitation precipitation frequency in the observations and the twelve
520 reanalysis twelve product reanalysis products (Fig. 4). Based on the observations, the
521 interannual variance of variations in T_a is are jointly determined by precipitation
522 frequency the frequency of precipitation precipitation frequency and L_d in Northeast
523 China and the northern part of Northwest China (Fig. 4). All of the reanalyses roughly
524 capture these factors over these regions, even although having they display
525 differences in the relative magnitudes (Fig. 4). Specifically, i.e., ERA-20CM, NOAA
526 20CRv2c, NOAA 20CRv2 and CFSR exhibit comparably comparable relationships of
527 T_a with precipitation frequency the frequency of precipitation precipitation frequency
528 and L_d , but; however, MERRA, MERRA2, NCEP-R2, ERA-20C, and CERA-20C
529 exhibit overestimated overestimate the relationships of between T_a with and
530 precipitation frequency the frequency of precipitation precipitation frequency, and
531 ERA-Interim, JRA-55, and NCEP-R1 present overestimated overestimate the

532 relationships of T_a with L_d over these regions (Fig. 4).

533 Over the North China Plain and Middle China, the interannual variance
534 of variations in T_a is are jointly determined by R_s , the precipitation frequency the
535 frequency of precipitation precipitation frequency and L_d (Fig. 4). The reanalyses
536 roughly capture the effects of these three factors on T_a , despite of, although they
537 display diverse combinations (Fig. 4). Among these combinations, the JRA-55,
538 MERRA2, ERA-20CM and ERA-Interim is are comparable to the observations over
539 these regions (Fig. 4). Over Southeast China, the interannual variance of variations in
540 T_a is are primarily regulated by L_d , the precipitation frequency the frequency of
541 precipitation precipitation frequency and R_s (Fig. 4). The reanalyses exhibit slightly
542 overestimated relationships of T_a with R_s and underestimated relationships with the
543 precipitation frequency the frequency of precipitation precipitation frequency (Fig. 4).

544 Over Tibetan Over the Tibetan Plateau, the interannual variance of variations in T_a
545 is are regulated by R_s and the precipitation frequency the frequency of
546 precipitation precipitation frequency (Fig. 4). Most reanalyses Most of the reanalyses
547 roughly capture the combinations of these factors, but exhibit a certain difference in
548 the relative impact effects of R_s and the precipitation frequency the frequency of
549 precipitation precipitation frequency on T_a (Fig. 4). MERRA, MERRA2, NOAA
550 20CRv2c and NOAA 20CRv2 overestimate the relationships of T_a with R_s over
551 Tibetan over the Tibetan Plateau (Fig. 4).

552 Overall, the spatial patterns of the simulated partial correlation of T_a with R_s in
553 the reanalysis products are significantly correlated with those from seen in the

554 observations ($r=0.13-0.35$, $p<0.05$) for the NWP-like reanalysis and larger
555 values of $r=0.24-0.41$, ($p<0.05$) are obtained for the climate reanalysis and.
556 Moreover, the spatial patterns in the sensitivity of T_a to R_s exhibit the significant
557 correlations ($r=0.12-0.17$, $p<0.05$) for most climate reanalyses most of the climate
558 reanalyses ($r=0.12-0.17$, $p<0.05$) (Table 1). The frequency of
559 precipitation frequency T displays the largest spatial correlations
560 ($r=0.16-0.43$, $p<0.05$) of the sensitivity of T_a to with these three relevant parameters
561 in the reanalyses is found to the precipitation frequency ($r=0.16-0.43$, $p<0.05$) (Table
562 3). The significant spatial correlations reflecting the relationships (including the
563 partial correlation and sensitivity) of T_a with L_d were also found (Table 1).

564 3.4 Regional Warming Trend Biases and Their Causes

565 From 1979 to 2010 over China, The T_a exhibits strong warming trends of
566 $0.37-0.7^{\circ}\text{C}/\text{decade}$ ($p<0.05$) from the observations and $0.22-0.48-0.8^{\circ}\text{C}/\text{decade}$
567 ($p<0.05$) among in the twelve reanalyses from 1979 to 2010 over China (Figs. 5 and
568 S2-S3, Table 2). The ERA-Interim and JRA-55 have display spatial correlations with
569 the observations ($r=0.47$ and 0.54 , $p<0.05$) that are due at least partly due to the
570 inclusion of some T_a observations, whereas NCEP-R2 and ERA-20C perform display
571 the worst performance (Figs. S3, Tables 1 and 3). Furthermore, approximately 87% of
572 the observed trends in T_a trend over China can be explained by the greenhouse effect
573 (i.e., 65% can be explained by the trend in L_d , 65%), the precipitation frequency the
574 frequency of precipitation precipitation frequency (29%) and R_s (-7%, due to the trend
575 in radiative forcing of $-1.1 \text{ W}\cdot\text{m}^{-2}/\text{decade}$) (Figs. S3-4). The influence of the

576 greenhouse effect off the observed trends in T_a trend mainly consists mainly of the
577 trends in the atmospheric water vapor (42%) and the cloud fraction (3%) (Fig. S5).
578 Among the reanalyses, over 90% of the T_a -trend in T_a can be explained by
579 greenhouse by the greenhouse effect, the precipitation frequency the frequency of
580 precipitation precipitation frequency and R_s (Figs. S4-6). Specifically, ERA-Interim,
581 JRA-55, MERRA and MERRA2 present display the best ability of capturing to capture
582 these contributions of the greenhouse effect (48% to 76%), the frequency of
583 precipitation precipitation frequency (22% to 34%) and R_s (-4% to 13%) to the T_a
584 trend trend in T_a over China, from greenhouse effect (48% to 76%), the precipitation
585 frequency (22% to 34%) and R_s (-4% to 13%) (Figs. S4 and S6). The remaining
586 NWP-like reanalyses (i.e., NCEP-R1 and NCEP-R2) largely substantially
587 overestimate the contribution of the R_s to the T_a -trend trend in T_a , whereas the
588 climate reanalyses overestimate the contribution that from the L_d (Figs. S4 and S6).

589 However, the averaged trends across a large territory over large areas may mask
590 regionally different regional differences values, reflecting that reflect diverse regional
591 warming biases and their causes (Figs. 5-7). Evidently, The mean-adjusted spatial
592 patterns of the trend biases in biases in the trends in T_a show consistency appear to be
593 consistent among the twelve reanalyses (Fig. S7) and mimic the spatial patterns in the
594 overestimated R_s trends over the North China Plain, South China and Northeast China
595 (Fig. S8), with given their spatial correlations between these variables in most
596 reanalyses most of the reanalyses ($r=0.11-0.42$, $p<0.05$) (Figs. 6 and S7-8, Table 3).
597 Howbeit However, the reanalyses still underestimate the T_a -trend trends in T_a over most

598 ~~of the regions, one of important reasons for which. The key reason for this~~
599 ~~underestimation is is~~ the increase in ~~precipitation frequency~~~~the frequency of~~
600 ~~precipitation~~~~precipitation frequency~~ over Northwest China, the Loess Plateau, ~~and~~
601 Middle China ~~for seen in~~ the NWP-like reanalyses and ~~that seen~~ over ~~boader~~~~broader~~
602 regions ~~for in the~~ climate reanalyses (Figs. 5-6 and S9). This ~~relationship~~ is reflected
603 by their negative spatial correlation ~~with which has~~ a maximum ~~value~~ of -0.62
604 ($p<0.05$)~~for~~ for MERRA~~3~~ (Table 3). Moreover, the decrease in L_d , ~~which occurs~~ due to
605 the decreases in the atmospheric water vapor and cloud fraction ~~that occur~~ in the
606 NWP-like reanalyses (Figs. S10-12), substantially cancels the warming effect of the
607 ~~everestimated overestimation of~~ R_s on T_a over eastern China (Figs. 5 and S7). The
608 opposite changes occur over Southeastern China in ~~the~~ climate reanalyses (Figs. 5 and
609 S10). ~~This The~~ effect of ~~the~~ changes in L_d is reflected by ~~their its~~ spatial correlations
610 of up to 0.50 ($p<0.05$) (Table 3).

611 Here, we further ~~quantified quantify the~~ contributions ~~of to the trend biases~~
612 ~~in biases in the trend in~~ T_a ~~made~~ by those in R_s , L_d and ~~the precipitation frequency~~~~the~~
613 ~~frequency of precipitation~~~~precipitation frequency~~ among the twelve reanalyses over
614 China and its seven subregions (Figs. 6-7). Over China, ~~the~~ overestimated R_s trends
615 (by $0.00\text{-}3.93 \text{ W}\cdot\text{m}^{-2}/\text{decade}$, ~~Fig;~~ ~~Fig.~~ S8 and S13) ~~can~~ increase the ~~T_a trend~~~~trends~~
616 ~~in T_a~~ (by $0.02\text{-}0.16 \text{ }^\circ\text{C}/\text{decade}$, ~~Fig;~~ ~~Fig.~~ 7) ~~in twelve~~~~in the twelve~~ reanalyses; ~~the~~,
617 underestimated L_d trends (by -0.25 to -1.61 $\text{W}\cdot\text{m}^{-2}/\text{decade}$ for the NWP-like
618 reanalyses, ~~Fig;~~ ~~Fig.~~ S10 and S15) ~~can~~ decrease the ~~T_a trend~~~~trends in T_a~~ (by -0.05 to
619 -0.25 $\text{ }^\circ\text{C}/\text{decade}$ for the NWP-like reanalyses, ~~Fig;~~ ~~Fig.~~ 7); and ~~the biases in~~

620 ~~precipitation frequency~~the trends in the frequency of precipitation
621 ~~frequency trends biases~~ (by approximately -1.5 days/decade for the NWP-like
622 reanalyses and approximately 2.6 days/decade for ~~the~~ climate reanalyses,~~Fig.~~Fig.
623 S9 and S14) ~~can~~ decrease the ~~T_a trend~~trends in T_a (by 0.01 to 0.05 °C/decade for the
624 NWP-like reanalyses and -0.01 to -0.06 °C/decade for ~~the~~ climate reanalyses,~~Fig.~~Fig.
625 7), ~~which jointly. Together, these effects produce an underestimate in the make the T_a~~
626 ~~trend~~trends in T_a ~~underestimated by~~on the order of 0.10 °C/decade ~~in reanalysis in the~~
627 ~~reanalyses~~ (Fig. 7 and Table 2).

628 Over northern China, ~~trend biases in biases in the trend in T_a primarily~~ result
629 ~~primarily~~ from those in ~~precipitation frequency~~the frequency of
630 ~~precipitation~~precipitation frequency and L_d (Figs. 6-7). Over Northeast China,
631 ~~observations, the observations~~ exhibit an amplified warming of 0.41-0.48 °C/decade
632 ($p < 0.05$,~~Fig.~~Fig. 4 and Table 2), ~~which. This warming~~ is significantly underestimated
633 by NCEP-R1, JRA-55, NOAA 20CRv2 and NOAA 20CRv2c (by ~~on~~ the order of
634 -0.15 °C/decade) and is overestimated by MERRA and CFSR (by ~~on~~ the order of
635 0.2 °C/decade) (Figs. 6-7). These ~~T_a trend biases~~bias in the trends in T_a in reanalysis in
636 ~~the reanalysis~~ are jointly explained ~~with~~by the warming (0.04-0.48 °C/decade)
637 induced by ~~the~~ underestimated trends in ~~precipitation frequency~~the frequency of
638 ~~precipitation~~precipitation frequency and the cooling (-0.04 to -0.42 °C/decade)
639 ~~induced~~ by ~~the~~ underestimated trends in L_d (Fig. 7).

640 Over Northwest China, ~~the trend biases in biases in the trend in precipitation~~
641 ~~frequency~~the frequency of precipitation and L_d ~~are~~ mainly

带格式的：缩进：左 0 字符，首行缩进： 0 字符

642 explained by the overestimated warming in NCEP-R2 (by 0.22 °C/decade) (Fig. 7).
643 Largely The substantially underestimated trend in L_d induced by the decrease in the
644 atmospheric water vapor and cloud fraction (Figs. S9-S12 and S16-17), leads to an
645 underestimating underestimate of the warming in MERRA (by -0.22 °C/decade) (Fig.
646 7).

647
648 Most reanalyses Most of the reanalyses present a display weakening weakened
649 warming over Tibetan over the Tibetan Plateau and the Loess Plateau (Fig. 5 and S3,
650 Table 2). More evidently In particular, NCEP-R1 and NCEP-R2 fail to reproduce the
651 warming over Tibetan over the Tibetan Plateau, and MERRA fails to reproduce the
652 warming over the Loess Plateau (Fig. 5 and S3, Table 2). The significant cooling trend
653 biases in biases in the trends in T_a (by -0.02 to -0.31 °C/decade) over the Tibetan
654 Plateau and Loess Plateau and the Loess Plateau result from the underestimating trends
655 in L_d and the overestimated trends in precipitation frequency the frequency of
656 precipitation precipitation frequency seen in most reanalyses most of the reanalyses (Figs.
657 5-7 and S9-12). This These cooling biases are further induced by the underestimating
658 trends in R_s (Figs. 5-7 and S8).

659 Over southern China, the trend biases in biases in the trend in T_a are regulated by
660 the trend biases in the trends those in R_s , L_d and the precipitation frequency the
661 frequency of precipitation precipitation frequency (Figs. 6-7). Over Southeast China,
662 the significantly overestimated significant overestimated trends in T_a (by
663 0.04, 0.02 and 0.17 °C/decade, respectively) are induced by the by overestimated

带格式的：缩进：左 0 字符，首行缩进： 0 字符

664 trends in R_s (by 4.25, 3.34 and $6.27 \text{ W}\cdot\text{m}^{-2}/\text{decade}$, respectively) seen in ERA-Interim,
665 JRA-55 and CFSR (Figs. 6-7 and S8). The underestimated ~~trends in T_a~~
666 induced by ~~the~~ overestimated trends in ~~precipitation frequency~~
667 ~~the frequency of precipitation~~ and L_d in NCEP-R1, MERRA, ERA-20CM,
668 CERA-20C, NOAA 20CRv2 and NOAA 20CRv2c (Figs. 6-7 and S9).

669 Over Middle China, ~~the significant oversignificantly over~~estimated ~~trends in~~
670 ~~T_a~~
671 induced by ~~the~~ overestimated trends in R_s (by 2.09, 1.50, 2.59, 1.20 and 4.81
672 $\text{W}\cdot\text{m}^{-2}/\text{decade}$, respectively) seen in ERA-Interim, JRA-55, ERA-20C, ERA-20CM,
673 CERA-20C and CFSR (Figs. 6-7 and S8). The overestimated trends in ~~precipitation~~
674 ~~frequency~~
675 cooling in the ~~trends in T_a~~
676 MERRA (~~which reflects an induced bias in the trend of~~ -0.15 $^\circ\text{C}/\text{decade}$ ~~of the~~
677 ~~induced trend bias~~) over Middle China (Figs. 6-7 and S9).

678 Due to ~~the~~ underestimated trends in the atmospheric water vapor and ~~the~~ cloud
679 fraction (Figs. S11-12), ~~the underestimation of the~~ L_d is ~~underestimated to~~
680 ~~have produces~~ a cooling effect on the ~~T_a trend~~ trend in T_a (by -0.05 to -0.32 $^\circ\text{C}/\text{decade}$)
681 ~~in reanalysis in the reanalyses~~ over ~~the~~ North China Plain (Figs. 6-7 and S10). However,
682 due to the lack of inclusion of ~~the~~ plausible trends in aerosol loading, the substantial
683 increases in R_s ~~over North over the North~~ China Plain (Fig. S8) have a strong warming
684 effects on the ~~T_a trend~~ trends in T_a (by 0.01 to 0.21 $^\circ\text{C}/\text{decade}$) ~~in reanalysis in the~~
685 ~~reanalyses~~ (Figs. 6-7 and S8). The ~~trend biases in biases in the trends in precipitation~~

686 frequency~~the frequency of precipitation~~precipitation frequency (by~~of~~ approximately
687 -2.5~~days~~/decade for the NWP-like reanalyses and approximately 1.5~~days~~/decade for
688 some ~~of the~~ climate reanalyses) contribute some part of ~~the trend biases in~~biases in the
689 trends in T_a (by~~approximately~~ 0.05 °C/decade for the NWP-like reanalyses and
690 -0.03 °C/decade for ~~the~~ climate reanalyses).-

691

692 Overall, ~~the trend biases in~~biases in the trends in T_a ~~in reanalys~~in the reanalyses
693 can be substantially explained by those in L_d , ~~precipitation frequency~~the frequency of
694 ~~precipitation~~precipitation frequency and R_s , but ~~it varies this effect varies by~~
695 regionally~~s~~ (Figs. 6-7). Over northern China, ~~the trend biases in~~biases in the trend in
696 T_a (by~~order of~~(which are on the order of -0.12 °C/decade) primarily result primarily
697 from a combination of those in L_d (by~~order of~~(which are on the order of
698 -0.10 °C/decade) and ~~precipitation frequency~~the frequency of
699 ~~precipitation~~precipitation frequency (by~~order of~~(which are on the order of
700 0.05 °C/decade), with relatively small contributions from R_s (by~~order of~~(which are on
701 the order of -0.03 °C/decade). Over southern China, ~~the trend biases in~~biases in the
702 trend in T_a (by~~order of~~(which are on the order of -0.07 °C/decade) are caused by those
703 in R_s (by~~order of~~(which are on the order of 0.10 °C/decade), L_d (by~~order of~~(which are
704 on the order of -0.08 °C/decade) and ~~precipitation frequency~~the frequency of
705 ~~precipitation~~precipitation frequency (by~~order of~~(which are on the order of
706 -0.06 °C/decade) (Fig. S18). Note also that the ~~analyses incorporation~~ of the
707 ~~observation observed~~ changes ~~of in~~ surface air temperatures~~s~~ in ERA-Interim and

708 JRA-55 may bring introduce trend biases in biases into the trends in the output of T_a
709 values, but however, the use of partial correlation and regression analysis would lead
710 to their smaller impacts of the biases in these physical variables in quantifying their
711 contributions of the T_a trend biases to the trends in T_a by the physical variables above.

712 3.5 Spatial Linkages of Warming Trend Biases in the Warming Trends

713 among in the Twelve Reanalyses

714 By We next integrate integrating the relationships of the spatial patterns in the T_a
715 trend biases in the trends in T_a with those in R_s , L_d and precipitation
716 frequency the frequency of precipitation over China among in
717 the twelve reanalyses (Fig. 8), it was found. The results show that the trend biases
718 in biases in the trends in T_a show significant correlations with R_s ($r=0.80$, slope=0.06,
719 $p=0.09$) and, precipitation frequency the frequency of precipitation precipitation
720 frequency ($r=-0.83$, slope=-0.04, $p=0.02$) and L_d ($r=0.77$, slope=0.10, $p=0.10$) among
721 in the twelve reanalyses; if include the information onf these patterns is included.
722 Without considering When the spatial patterns of the trend biases in biases in the trends
723 in these variables are not considered, the T_a trend biases in biases in the trends in T_a show
724 relatively smaller correlations with R_s ($r=0.32$, slope=0.02, $p>0.1$), precipitation
725 frequency the frequency of precipitation precipitation frequency ($r=-0.51$, slope=-0.02,
726 $p=0.09$) and L_d ($r=0.14$, slope=0.02, $p>0.1$) among in the reanalyses (Fig. 8). The
727 same Similar circumstances occur results are obtained for the atmospheric water vapor
728 ($r=0.71$, $p=0.1$) and the cloud fraction ($r=-0.74$, $p=0.09$) if consider their spatial
729 patterns are considered (Figs. S19), and this relationship from involving the cloud

730 fraction is very similar to that from the associated with R_s (Figs. 8 and S19). Over
731 Within the China's subregions subregions of China, the trend biases in biases in the
732 trends in T_a show significant correlations with R_s ($r=0.68$ to 0.90 , $p<0.1$), precipitation
733 frequency the frequency of precipitation precipitation frequency ($r=-0.55$ to -0.94 ,
734 $p<0.1$) and L_d ($r=0.53$ to 0.93 , $p<0.1$) with when the inclusion f spatial patterns among
735 in the reanalyses are included (Fig. S20). These results provide a novel view
736 to perspective that can be used to investigate the spatial relationships between trend
737 biases in biases in the trends in T_a and the relevant quantities among in the reanalyses.

738

739 **4. Discussion**

740 In this section, we first examined the possible impacts of data homogenization on
741 the T_a trend trends in T_a . The T_a trend trends in T_a derived from the original dataset are
742 almost higher as high as than those from the homogenous data homogenized data set,
743 especially over the North China Plain and Northwest China (Fig. 5 and Table 2). This
744 Homogenization primarily adjusts the breakpoints in the time series (Wang, 2008),
745 which occur mainly due mainly due to station relocation and changes in instruments
746 (Cao et al., 2016; Li et al., 2017; Wang, 2014), and it helps to objectively depict the
747 T_a trend trends in T_a for thus permitting the assessment of the modelled T_a trend trends
748 in T_a and its spatial patterns that are present in the reanalyses.

749 We found that the elevation differences between the models and the stations
750 actually influence the biases in the T_a trend trends in T_a bias, but can but can not
751 explain the spatial patterns in the T_a trend the biases in the trends in T_a bias (averaged

752 $r=0.11$) (Fig. S21). Compared the same grid models Comparison of the models that
753 use the same grid (NOAA 20CRv2c vs. NOAA 20CRv2, MERRA vs. MERRA2,
754 NCEP-R1 vs. NCEP-R2 and ERA-20C vs. ERA-20CM), we found the shows that the
755 one is statistically correlated with elevation differences, but the other does not,
756 which implies that this statistical correlation should not be physical significance does
757 not have physical significance. Besides, In addition, elevation differences does not
758 change with time. Nevertheless, the spatial patterns in the normalized trends in
759 T_a (excluding the impacts of the absolute value of temperature on the
760 trends) are very near to those of the trends (Fig. S22), implying the impact of that the
761 differences in the absolute value of temperature have an important effect due to, given
762 that the site-to-grid inconsistency can be neglected.

763 In reanalyses In the reanalyses, vegetation is only included as a climatological
764 information, but the vegetation has displays a growth trend in nature during the study
765 period 1979-2010 over within China (Fig. S23), which. This discrepancy
766 will positively enlarges the T_a trend biases in the trends in T_a due to the
767 vegetation cooling effect (Zeng et al., 2017; Trigo et al., 2015). This effect is
768 reflected by the negative spatial correlation ($r=-0.26, p=0.00$) between the inverted
769 trend in the NDVI and the trend biases in the trend in T_a (Fig. S23). The
770 vegetation growth would growth of vegetation cool the reduces T_a near surface air
771 temperatures by regulating surface roughness, surface conductivity, soil moisture and
772 albedo to partition more greater amounts of available energy into latent heat fluxes
773 and then, which leads to the formation of more precipitation (Shen et al., 2015).

774 Spracklen et al., 2013), thereby. Thus, the inclusion of vegetation growth will have
775 improved effect on the improve the simulation of trend simulations (and especially for
776 the spatial pattern) of T_a in reanalyses through a the incorporation of
777 more complete physical parameterizations above in reanalysis (Li et al., 2005; Dee
778 and Todling, 2000; Trigo et al., 2015).

779 Due to their inclusion of surface air temperature observations, the ERA-Interim
780 and JRA-55 exhibit a relatively skillful pattern display high skill in reproducing the
781 observed patterns with; they have near-zero means (0.01 and 0.01 °C/decade) and the
782 smallest standard deviations (0.16 and 0.15 °C/decade) of the trend biases among the
783 twelve reanalyses twelve products, albeit being still evident.
784 However, pattern differences of 37.8% (standard deviation of trend
785 bias/China-averaged trend) are still evident (Figs. 5 and 8). Despite of no inclusion
786 of Although it does not incorporate surface air temperature observations, ERA-20CM
787 presents a pattern (with a mean of -0.04 °C/decade and a standard deviation of
788 0.15 °C/decade, Fig; Figs. 5 and 8) that is comparable to those of ERA-Interim and
789 JRA-55; and better than that of ERA-20C (mean of -0.08 °C/decade and standard
790 deviation of 0.20 °C/decade, Fig; Figs. 5 and 8) with, which uses the same forecast
791 model as ERA-20CM, which implies. These results imply that a potential approach of
792 ensemble forecasting could be used to meet to this end important goals. This
793 advantage of The ensemble forecasting technique used in ERA-20CM also displays
794 advantages in that it perform better in they yields an improved simulated pattern of
795 trend biases in R_s biases in the trends in R_s (SD=1.84 W m⁻²/decade, 171%),

796 precipitation frequency the frequency of precipitation precipitation frequency
797 (SD=2.78days/decade, 122%) and L_d (SD=1.25 W m⁻²/decade, 82%) (Fig. 8).

798 We considered to which extent the degree to which the ensemble assimilation
799 technique can improve the spatial patterns of the biases in the T_a trend trends in T_a bias
800 in reanalysis in the reanalyses. We found find that this technique can detect the T_a trend
801 biases biases in the trends in T_a over more another more another approximately 12%
802 (8%) of the grids grid cells for in CERA-20C with which incorporates 10 ensemble
803 members (NOAA 20CR2vc and NOAA 20CR2v with employ 56 ensemble
804 members) (Figs. 541-n). However, the T_a trend biases biases in the trends in T_a over
805 these grids grid cells were are detected to be not n significant at the a significance level
806 of 0.05, according to for Student's t-test, implying that the ensemble assimilation
807 technique can not explain the spatial pattern of the T_a trend biases biases in the trends
808 in T_a identified displayed in this study (in Figs. 541-n).

809 To preliminarily To provide a preliminary discussion of the improvements of in
810 climate forecast models in reflecting patterns in climate trends, we compare the
811 spatial patterns of the trend biases in R_s biases in the trends in R_s , precipitation
812 frequency the frequency of precipitation precipitation frequency and L_d without direct
813 observations analyzed in the reanalyses in the reanalyses that do not incorporate
814 observations. We can find that the climate forecast models, i.e., ERA-20C,
815 ERA-20CM, CERA-20C, NOAA 20CRv2c and NOAA 20CRv2, perform
816 better display better performance in reproducing the pattern of trend biases in R_s biases
817 in the trends in R_s (mean of 1.36 vs. 2.18 W m⁻²/decade; SD of 2.04 vs. 2.71

818 W m⁻²/decade), ~~precipitation frequency~~the frequency of precipitation
819 ~~frequency~~ (mean of 1.32 vs. -1.4~~4~~4%/decade; SD of 3.57 vs. 6.1~~4~~4%/decade)
820 and L_d (mean of 0.12 vs. -0.85 W m⁻²/decade; SD of 1.33 vs. 1.50 W m⁻²/decade)
821 than the NWP-like models, i.e., ERA-Interim, NCEP-R1, MERRA, JRA-55,
822 NCEP-R2 and MERRA2 (Fig. 8). ~~Besides,~~In addition, because the SST boundary
823 condition ~~freely~~ evolves ~~sd freely~~ in CFSR, the patterns of ~~trend biases in R_s~~ biases in
824 the trends in R_s , ~~precipitation frequency~~the frequency of precipitation
825 ~~frequency~~ and L_d in CFSR ~~substantially~~ differ substantially from those in the other
826 reanalyses.

827 We also ~~considered consider~~ whether the spatial pattern of ~~trend biases in~~biases in
828 ~~the trend in T_a~~ is altered by the atmospheric ~~circulations~~circulation patterns simulated
829 by the ERA-20CM ensembles. In ERA-20CM, the atmospheric ~~circulations~~circulation
830 patterns are influenced ~~from by~~ SSTs and sea ice and then partly mediate the
831 influences of global forcings on the ~~T_a trend~~trends in T_a . In ERA-20CM, the
832 probability distribution function of the ~~T_a trend biases~~biases in the trends in T_a from
833 outside the ensemble ranges incorporates that from Student's *t*-test at a significance
834 level of 0.05 (Fig. 5k). This result has important implications in that 1) the climate
835 variability in ~~the model~~ ensembles under the different model realizations of SSTs and
836 sea ice cover does not change the pattern of the ~~T_a trend biases~~biases in the trends in T_a
837 (Fig. 5k); ~~; moreover,~~ 2) A-Student's *t*-test exhibits a suitable ability to detect the
838 significance of the ~~T_a trend biases~~biases in the trends in T_a (Fig. 5k) ~~for when~~
839 considering the effects of interannual variability on the trend.

840 Overall, producing global or regional reanalyses that adequately reflect regional
841 climate is challenging using the current strategy, and further improvements are
842 required. The results and discussion above indicate some potential but challenging
843 approaches that can be used to maximize the signal component corresponding to the
844 regional climate in final reanalyses and robustly narrow the uncertainties in trends.

845 1) MERRA2 incorporates time-varying aerosol loadings in a pioneering attempt
846 to improve regional warming over the North China Plain to some extent. Thus, we
847 encourage research groups to include accurate aerosol information and improve the
848 skill of simulation of the energy budget and partitioning, especially of regional
849 surface incident solar radiation, in other reanalyses.

850 2) To improve regional climate modelling, forecast output should be produced
851 using a physical ensemble like that employed in ERA-20CM to quantify the
852 uncertainties associated with the relevant parameterizations in the reanalyses, due to
853 the impossibility of optimizing all of the biases. Meanwhile, careful ensemble design
854 would likely yield useful information for use in improving models, assimilation
855 methods and the bias correction of observations by exploring the interdependency
856 among sources of errors. Such designs would undoubtedly have additional benefits for
857 further development, leading to the next generation of reanalyses.

858 3) To improve coupled land-atmospheric interactions, the true dynamics of land
859 cover and use should be incorporated. Moreover, the physical parameterizations
860 should be improved, including the responses of surface roughness, surface
861 conductivity and albedo to regional climate. These changes would represent an

862 improvement over the use of constant types and fractions of vegetation, as is done in
863 ERA-Interim (Zhou and Wang, 2016a).

864 4) Given the implications of the spurious performance of the freely evolving
865 boundary conditions in CFSR, homogeneous and accurate records of SST and sea ice
866 should be produced.

867 Next-generation reanalyses, including both global and regional reanalyses, will
868 assimilate and analyse *in situ* observations, satellite radiance, and other remote
869 observations. In addition to short-term accuracy and long-term trends, they will also
870 focus on spatial patterns by incorporating or improving accurate representations of
871 land surface conditions and processes within the coupled weather and climate Earth
872 systems. Thus, these reanalyses will advance the simulation of land-atmosphere
873 interactions to yield high skill in studies of regional warming and the detection and
874 attribution of regional climate change using various datasets, which frequently include
875 global and regional reanalyses (Zhou et al., 2018; Zhou and Wang, 2016c; Herring et
876 al., 2018; Trenberth et al., 2015; Stott, 2016; Dai et al., 2017; Zhou and Wang, 2017b).
877 Additionally, the uncertainties associated with regional warming could be ascertained
878 using physics ensembles with various equiprobable realizations of boundary
879 conditions.

880

881 **45. Conclusions and Perspectives**

882 Reanalyses—The reanalyses have displayed differences in T_a referenced when
883 compared to the observations with a range of -10~10 °C over China—a. Approximately

884 74% and 6% of ~~which these differences~~ can be explained ~~by the~~ site-to-grid elevation
885 differences and the filtering error in ~~the elevations used in the~~ spectral models
886 ~~elevation. This These results implies imply~~a fairly good skill in the simulation of ~~the~~
887 climatology of T_a in the twelve reanalyses over China. Moreover, ~~the twelve~~
888 reanalyses roughly capture the interannual ~~variability of variability in~~ T_a ~~among the~~
889 ~~twelve reanalysis~~ (median $r=0.95$). ~~Reanalyses In the reanalyses, exhibit that~~ T_a has
890 ~~displays a~~ consistently positive correlations with ~~the~~ R_s and L_d , and ~~has is~~ negatively
891 ~~correlations correlated~~ with ~~precipitation frequency the frequency of~~
892 ~~precipitation precipitation frequency~~, as ~~those seen~~ in observations, despite ~~of~~
893 ~~having the~~ evident spatial patterns in their magnitudes over China.

894 ~~The~~ T_a exhibits a strong warming trend of $0.37 \pm 0.07 \text{ }^{\circ}\text{C}/\text{decade}$ ($p<0.05$) ~~from in~~
895 the observations and $0.22-0.48 \pm 0.08 \text{ }^{\circ}\text{C}/\text{decade}$ ($p<0.05$) ~~among in~~ the twelve
896 reanalyses over China. In ~~the~~ observations, ~~approximately 87% of the observed trend~~
897 ~~in T_a over China can be explained by the greenhouse effect (i.e., 65% can be~~
898 ~~explained by the trend in L_d), the frequency of precipitation precipitation frequency~~
899 ~~(29%) and R_s (-7%, due to the trend in radiative forcing of -1.1~~
900 ~~$\text{W} \cdot \text{m}^{-2}/\text{decade}$) approximately 87% of the observed T_a trend can be explained by~~
901 ~~greenhouse effect (i.e., trend in L_d , 65%), the precipitation frequency (29%) and R_s~~
902 ~~(-7%, due to the trend of $-1.1 \text{ W} \cdot \text{m}^{-2}/\text{decade}$) over China.~~

903 However, the ~~trends biases in biases in the trends in~~ T_a ~~from seen in the~~ reanalyses
904 ~~relative~~ to the observations display an evident spatial pattern
905 (mean= $-0.16 \pm 0.11 \text{ }^{\circ}\text{C}/\text{decade}$, SD= $0.15-0.30 \text{ }^{\circ}\text{C}/\text{decade}$). The spatial patterns of the

906 ~~trends biases in~~biases in the trends in the values of reanalyzed T_a in the reanalyses
907 ~~have significant correlations~~are significantly correlated with those in R_s (maximum r
908 $=0.42$, $p<0.05$), ~~precipitation frequency~~the frequency of precipitation
909 ~~frequency~~ (maximum $r=-0.62$, $p<0.05$) and L_d (maximum $r=-0.50$, $p<0.05$). Over
910 northern China, the ~~trend biases in~~biases in the trends in T_a (~~by order of~~which are on
911 ~~the order of~~ -0.12 °C/decade) ~~primarily~~ result primarily from a combination of those in
912 L_d (~~by order of~~which are on the order of -0.10 °C/decade) and ~~precipitation~~
913 ~~frequency~~the frequency of precipitation~~precipitation frequency~~ (~~by order of~~which are
914 ~~on the order of~~ 0.05 °C/decade), with relatively small contributions~~s~~ from R_s (~~by order~~
915 ~~of~~which are on the order of -0.03 °C/decade). Over southern China, the ~~trend biases~~
916 ~~in~~biases in the trends in T_a (~~by order of~~which are on the order of -0.07 °C/decade) are
917 regulated by the ~~trend~~ biases ~~those in the trends~~ in R_s (~~by order of~~which are on the
918 ~~order of~~ 0.10 °C/decade), L_d (~~by order of~~which are on the order of -0.08 °C/decade)
919 and ~~the precipitation frequency~~the frequency of precipitation~~precipitation frequency~~
920 (~~by order of~~which are on the order of -0.06 °C/decade).

921 If ~~include~~ information on~~f~~ spatial patterns is included, the simulated ~~trend biases~~
922 ~~of~~biases in the trends in T_a correlate well with those of ~~precipitation frequency~~the
923 ~~frequency of precipitation~~precipitation frequency, R_s and L_d ~~among in~~ the reanalyses
924 ($r=-0.83$, 0.80 and 0.77, $p<0.1$), ~~so they are; similar results are obtained~~ for the
925 atmospheric water vapor and ~~the~~ cloud fraction ($r=0.71$ and -0.74, $p<0.1$). These
926 results provide a novel ~~view to~~perspective that can be used to investigate the spatial
927 relationships~~s~~ between the ~~trend biases in~~biases in the trends in T_a and the relevant

928 parameters among the twelve reanalyses.

929 ~~From the observation, model and assimilation method, we comprehensively~~
930 ~~discussed their possible impact on the simulated biases in spatial pattern of the T_a~~
931 ~~trends. Overall, it's a challenge to produce a global or regional reanalysis suitable for~~
932 ~~region climate under the current strategy and to do improvement. Based on the results~~
933 ~~above, some potential but challenging approaches arise to maximize regional climate~~
934 ~~signal component in the final reanalysis and robustly narrow the trend uncertainties:~~

935 ~~1) As a pioneer, MERRA2 tried to incorporate time varying aerosol loadings to~~
936 ~~improve regional warming over the North China Plain to some extent, so encourage to~~
937 ~~assimilate the accurate aerosol information and improve simulated skill of energy~~
938 ~~budget and partitioning, especially for regional surface incident solar radiation in the~~
939 ~~other reanalyses.~~

940 ~~2) Make use of precipitation datasets with high temporal resolution from *in situ*~~
941 ~~and satellite based observations (Zhou and Wang, 2017a; Trenberth and Zhang,~~
942 ~~2017; Dai et al., 2017) or the GPS water vapor (Bengtsson et al., 2003; Veen~~
943 ~~2017; Poli et al., 2010) to dynamically constrain precipitation occurrence including~~
944 ~~precipitation intensity and frequency (Qian et al., 2006; Trenberth et al.,~~
945 ~~2011; Bengtsson et al., 2007; Trenberth, 2004). This, in turn, will have more accurate~~
946 ~~representations of clouds and precipitation, especially their responses to climate~~
947 ~~change (Dai et al., 2017; Zhou and Wang, 2017b).~~

948 ~~3) Produce forecast output using a perturbed physical ensemble like ERA 20CM~~
949 ~~to quantify the uncertainty associated with relevant parameterizations in reanalyses,~~

950 due to impossibility to optimize all the biases to improve regional climate modeling.
951 Meanwhile, careful ensemble design would probably yield useful information to
952 improve model/assimilation and bias correction of observation by exploring
953 interdependency among sources of errors. They would undoubtedly have additional
954 benefit for further development pathways to the next generation of reanalyses.

955 4) Incorporate the true dynamics of land cover and use and improve the physical
956 parameterizations such as the response of surface roughness, surface conductivity and
957 albedo to regional climates, rather than constant type and fraction of vegetation as
958 ERA Interim (Zhou and Wang, 2016a), to improve the coupling of land-atmospheric
959 interaction.

960 5) Implication from the spurious performance of freely evolved boundary
961 conditions in CFSR, the homogeneous SST/sea ice should be reconstructed by
962 bringing together many previous versions and new ARGO ocean observing network.

963 A next-generation reanalysis including global and regional reanalyses will have
964 focus not only on short-term accuracy and long-term trends by assimilating *in-situ*
965 observations, satellite radiances, and other remote observations, but also on their
966 spatial patterns by incorporating or improving accurate representations of land surface
967 conditions and processes within unified weather-climate coupled Earth systems, to
968 advance the simulation of the land-atmosphere interactions for good skill in regional
969 warming studies, so as for the detection and attribution of regional climate changes
970 using various datasets and global/regional reanalyses widely included (Zhou et al.,
971 2018; Zhou and Wang, 2016c; Herring et al., 2018; Trenberth et al., 2015; Stott,

972 ~~2016; Dai et al., 2017; Zhou and Wang, 2017b). Additionally, the uncertainties of~~
973 ~~regional warming could be ascertained by perturbed model physics ensembles with~~
974 ~~various equiprobable realizations of boundary conditions.~~

975 Therefore, improving simulations of ~~precipitation frequency~~the frequency of
976 ~~precipitation~~precipitation frequency and R_s helps to maximize ~~the regional climate~~
977 ~~signal component~~signal component corresponding to the regional climate. Besides, In
978 addition, incorporating vegetation dynamics ~~in reanalysis~~in reanalyses and the use of
979 accurate aerosol information, ~~as~~ in MERRA-2 (~~Modern Era Retrospective Analysis~~
980 ~~for Research and Applications, version 2~~, would advance ~~the regional warming~~
981 ~~modeling~~modelling of regional warming. Ensemble ~~The ensemble~~ technique (adopted
982 in ERA-20CM, a ~~twentieth-century~~twentieth-century atmospheric model ensemble
983 ~~without assimilating observations~~)that does not assimilate observations, significantly
984 narrows ~~the regional warming uncertainties~~uncertainties of regional warming ~~in~~
985 reanalysis~~in the reanalyse~~is (standard deviation=0.15 °C/decade).

986

987 **Acknowledgements** This study ~~was~~was funded by the National Key R&D Program
988 of China (2017YFA0603601) and, the National Natural Science Foundation of China
989 (41525018). The latest ~~observation~~observational ~~data~~datasets ~~were~~were obtained
990 from the China Meteorological Administration (CMA;<http://www.cma.gov.cn>).
991 Considerable gratitude is owed to several reanalysis working teams, including the
992 European Centre for Medium-Range Weather Forecasts (ECMWF) for providing the
993 ERA-Interim, ERA-20C, ERA-20CM and CERA-20C data (<http://www.ecmwf.int/>);

994 the Global ~~ModelingModelling~~ and Assimilation Office (GMAO) at the NASA
995 Goddard Space Flight Center for providing the MERRA and MERRA2 data
996 (<http://gmao.gsfc.nasa.gov/>)~~for~~the the NOAA Earth System Research Laboratory (ESRL)
997 for providing the NCEP-R1, NCEP-R2, CFSR~~for~~the NOAA 20CRv2 and NOAA 20CRv2c
998 data (<http://www.esrl.noaa.gov/>)~~for~~the and the Climate Prediction Division of the Global
999 Environment and Marine Department at the Japan Meteorological Agency for
1000 providing the JRA-55 data (<http://jra.kishou.go.jp/>). We thank the Expert Team on
1001 Climate Change Detection and Indices (ETCCDI) for providing the RHtestV4
1002 package (<http://etccdi.pacificclimate.org/software.shtml>), the United States
1003 Geological Survey Earth Resources Observation and Science Data Center for
1004 providing the GTOPO30 data
1005 (<http://edc.usgs.gov/products/elevation/gtopo30/gtopo30.html>) and the working team
1006 ~~for of~~ the Global Inventory Monitoring and ~~ModelingModelling~~ System (GIMMS)
1007 project (<https://ecocast.arc.nasa.gov/data/pub/gimms/>). We thank Kevin E. Trenberth
1008 for his insightful suggestions.

1009 **References**

- 1010 Aarnes, O. J., Abdalla, S., Bidlot, J.-R., and Breivik, Ø.: Marine wind and wave
1011 height trends at different ERA-Interim forecast ranges, *J. Clim.*, 28, 819-837,
1012 10.1175/jcli-d-14-00470.1, 2015.
- 1013 Andersson, E., Bauer, P., Beljaars, A., Chevallier, F., Holm, E., Janiskova, M.,
1014 Kallberg, P., Kelly, G., Lopez, P., McNally, A., Moreau, E., Simmons, A. J., Thepaut,
1015 J. N., and Tompkins, A. M.: Assimilation and modeling of the atmospheric
1016 hydrological cycle in the ECMWF forecasting system, *Bull. Am. Meteorol. Soc.*, 86,
1017 387-402, 10.1175/bams-86-3-387, 2005.
- 1018 Balsamo, G., Albergel, C., Beljaars, A., Boussetta, S., Brun, E., Cloke, H., Dee, D.,
1019 Dutra, E., Muñoz-Sabater, J., Pappenberger, F., de Rosnay, P., Stockdale, T., and Vitart,
1020 F.: ERA-Interim/Land: a global land surface reanalysis data set, *Hydrol. Earth Syst.
1021 Sci.*, 19, 389-407, 10.5194/hess-19-389-2015, 2015.
- 1022 Bauer, P., Thorpe, A., and Brunet, G.: The quiet revolution of numerical weather
1023 prediction, *Nature*, 525, 47-55, 10.1038/nature14956, 2015.
- 1024 Bengtsson, L., Kanamitsu, M., Kallberg, P., and Uppala, S.: FGGE research activities
1025 at ECMWF, *Bull. Am. Meteorol. Soc.*, 63, 227-303, 1982a.
- 1026 Bengtsson, L., Kanamitsu, M., Kallberg, P., and Uppala, S.: FGGE 4-dimensional data
1027 assimilation at ECMWF, *Bull. Am. Meteorol. Soc.*, 63, 29-43, 1982b.
- 1028 Bengtsson, L., and Shukla, J.: Integration of space and in situ observations to study
1029 global climate change, *Bull. Am. Meteorol. Soc.*, 69, 1130-1143,
1030 10.1175/1520-0477(1988)069<1130:iosais>2.0.co;2, 1988.
- 1031 Bengtsson, L., Robinson, G., Anthes, R., Aonashi, K., Dodson, A., Elgered, G., Gendt,
1032 G., Gurney, R., Jietai, M., and Mitchell, C.: The use of GPS measurements for water
1033 vapor determination, *Bull. Am. Meteorol. Soc.*, 84, 1249-1258, 2003.
- 1034 Bengtsson, L., Hagemann, S., and Hodges, K. I.: Can climate trends be calculated
1035 from reanalysis data?, *J Geophys Res-Atmos.*, 109, D11111, 10.1029/2004jd004536,
1036 2004.
- 1037 Bengtsson, L., Haines, K., Hodges, K. I., Arkin, P., Berriesford, P., Bougeault, P.,
1038 Kallberg, P., Simmons, A. J., Uppala, S., Folland, C. K., Gordon, C., Rayner, N.,
1039 Thorne, P. W., Jones, P., Stammer, D., and Vose, R. S.: The need for a dynamical
1040 climate reanalysis, *Bull. Am. Meteorol. Soc.*, 88, 495-501, 10.1175/bams-88-4-495,
1041 2007.
- 1042 Betts, A. K., Hong, S.-Y., and Pan, H.-L.: Comparison of NCEP-NCAR reanalysis
1043 with 1987 FIFE data, *Monthly Weather Review*, 124, 1480-1498,
1044 10.1175/1520-0493(1996)124<1480:connrw>2.0.co;2, 1996.

- 1045 Betts, A. K., Viterbo, P., and Beljaars, A. C. M.: Comparison of the land-surface
1046 interaction in the ECMWF reanalysis model with the 1987 FIFE data, *Monthly*
1047 *Weather Review*, 126, 186-198, 10.1175/1520-0493(1998)126<0186:cotsi>2.0.co;2,
1048 1998.
- 1049 Betts, A. K.: Understanding hydrometeorology using global models, *Bull. Am.*
1050 *Meteorol. Soc.*, 85, 1673-1688, 10.1175/bams-85-11-1673, 2004.
- 1051 Bilbao, J., and De Miguel, A. H.: Estimation of daylight downward longwave
1052 atmospheric irradiance under clear-sky and all-sky conditions, *J. Appl. Meteor.*
1053 *Climatol.*, 46, 878-889, 2007.
- 1054 Brunt, D.: Notes on radiation in the atmosphere. I, *Q. J. Roy. Meteorol. Soc.*, 58,
1055 389-420, 1932.
- 1056 Buizza, R., Poli, P., Rixen, M., Alonso-Balmaseda, M., Bosilovich, M. G.,
1057 Brönnimann, S., Compo, G. P., Dee, D. P., Desiato, F., Doutriaux-Boucher, M.,
1058 Fujiwara, M., Kaiser-Weiss, A. K., Kobayashi, S., Liu, Z., Masina, S., Mathieu, P.-P.,
1059 Rayner, N., Richter, C., Seneviratne, S. I., Simmons, A. J., Thépaut, J.-N., Auger, J. D.,
1060 Bechtold, M., Berntell, E., Dong, B., Kozubek, M., Sharif, K., Thomas, C.,
1061 Schimanke, S., Storto, A., Tuma, M., Väistö, I., and Vaselali, A.: Advancing Global
1062 & Regional Reanalyses, *Bull. Am. Meteorol. Soc.*, published online,
1063 10.1175/bams-d-17-0312.1, 2018.
- 1064 Cao, L., Zhu, Y., Tang, G., Yuan, F., and Yan, Z.: Climatic warming in China
1065 according to a homogenized data set from 2419 stations, *Int. J. Climatol.*, 36,
1066 4384-4392, 10.1002/joc.4639, 2016.
- 1067 Cash, B. A., III, J. L. K., Adams, J., Altshuler, E., Huang, B., Jin, E. K., Manganello,
1068 J., Marx, L., and Jung, T.: Regional structure of the Indian summer monsoon in
1069 observations, reanalysis, and simulation, *J. Clim.*, 28, 1824-1841,
1070 10.1175/jcli-d-14-00292.1, 2015.
- 1071 Chen, J., Del Genio, A. D., Carlson, B. E., and Bosilovich, M. G.: The spatiotemporal
1072 structure of twentieth-century climate variations in observations and reanalyses. Part I:
1073 Long-term trend, *J. Clim.*, 21, 2611-2633, 2008.
- 1074 Choi, M., Jacobs, J. M., and Kustas, W. P.: Assessment of clear and cloudy sky
1075 parameterizations for daily downwelling longwave radiation over different land
1076 surfaces in Florida, USA, *Geophys. Res. Lett.*, 35, L20402, 2008.
- 1077 Compo, G. P., Whitaker, J. S., Sardeshmukh, P. D., Matsui, N., Allan, R. J., Yin, X.,
1078 Gleason, B. E., Vose, R. S., Rutledge, G., Bessemoulin, P., Brönnimann, S., Brunet,
1079 M., Crouthamel, R. I., Grant, A. N., Groisman, P. Y., Jones, P. D., Kruk, M. C., Kruger,
1080 A. C., Marshall, G. J., Maugeri, M., Mok, H. Y., Nordli, Ø., Ross, T. F., Trigo, R. M.,
1081 Wang, X. L., Woodruff, S. D., and Worley, S. J.: The twentieth century reanalysis

- 1082 project, Q. J. Roy. Meteorol. Soc., 137, 1-28, 10.1002/qj.776, 2011.
- 1083 Compo, G. P., Sardeshmukh, P. D., Whitaker, J. S., Brohan, P., Jones, P. D., and
1084 McColl, C.: Independent confirmation of global land warming without the use of
1085 station temperatures, Geophys. Res. Lett., 40, 3170-3174, 2013.
- 1086 Cornes, R. C., and Jones, P. D.: How well does the ERA-Interim reanalysis replicate
1087 trends in extremes of surface temperature across Europe?, J Geophys Res-Atmos, 118,
1088 10262-10276, 10.1002/jgrd.50799, 2013.
- 1089 Dai, A., Wang, J., Thorne, P. W., Parker, D. E., Haimberger, L., and Wang, X. L.: A
1090 new approach to homogenize daily radiosonde humidity data, J. Clim., 24, 965-991,
1091 10.1175/2010jcli3816.1, 2011.
- 1092 Dai, A., Rasmussen, R. M., Liu, C., Ikeda, K., and Prein, A. F.: A new mechanism for
1093 warm-season precipitation response to global warming based on
1094 convection-permitting simulations, Clim. Dyn., published online,
1095 10.1007/s00382-017-3787-6, 2017.
- 1096 Dee, D. P., and Da Silva, A. M.: Data assimilation in the presence of forecast bias, Q.
1097 J. Roy. Meteorol. Soc., 124, 269-295, 1998.
- 1098 Dee, D. P., and Todling, R.: Data assimilation in the presence of forecast bias: The
1099 GEOS moisture analysis, Monthly Weather Review, 128, 3268-3282,
1100 10.1175/1520-0493(2000)128<3268:daitpo>2.0.co;2, 2000.
- 1101 Dee, D. P.: Bias and data assimilation, Q. J. Roy. Meteorol. Soc., 131, 3323-3343,
1102 2005.
- 1103 Dee, D. P., and Uppala, S.: Variational bias correction of satellite radiance data in the
1104 ERA-Interim reanalysis, Q. J. Roy. Meteorol. Soc., 135, 1830-1841, 10.1002/qj.493,
1105 2009.
- 1106 Dee, D. P., Källén, E., Simmons, A. J., and Haimberger, L.: Comments on
1107 “Reanalyses suitable for characterizing long-term trends”, Bull. Am. Meteorol. Soc.,
1108 92, 65-70, 10.1175/2010BAMS3070.1, 2011a.
- 1109 Dee, D. P., Uppala, S. M., Simmons, A. J., Berrisford, P., Poli, P., Kobayashi, S.,
1110 Andrae, U., Balmaseda, M. A., Balsamo, G., Bauer, P., Bechtold, P., Beljaars, A. C.
1111 M., van de Berg, L., Bidlot, J., Bormann, N., Delsol, C., Dragani, R., Fuentes, M.,
1112 Geer, A. J., Haimberger, L., Healy, S. B., Hersbach, H., Hódmezői, E. V., Isaksen, L.,
1113 Källberg, P., Köhler, M., Matricardi, M., McNally, A. P., Monge-Sanz, B. M.,
1114 Morcrette, J. J., Park, B. K., Peubey, C., de Rosnay, P., Tavolato, C., Thépaut, J. N.,
1115 and Vitart, F.: The ERA-Interim reanalysis: configuration and performance of the data
1116 assimilation system, Q. J. Roy. Meteorol. Soc., 137, 553-597, 10.1002/qj.828, 2011b.
- 1117 Dee, D. P., Balmaseda, M., Balsamo, G., Engelen, R., Simmons, A. J., and Thépaut, J.

- 1118 N.: Toward a consistent reanalysis of the climate system, Bull. Am. Meteorol. Soc., 95,
1119 1235-1248, 10.1175/bams-d-13-00043.1, 2014.
- 1120 Desroziers, G., Berre, L., Chapnik, B., and Poli, P.: Diagnosis of observation,
1121 background and analysis - error statistics in observation space, Q. J. Roy. Meteorol.
1122 Soc., 131, 3385-3396, 2005.
- 1123 Dolinar, E. K., Dong, X., and Xi, B.: Evaluation and intercomparison of clouds,
1124 precipitation, and radiation budgets in recent reanalyses using satellite-surface
1125 observations, Clim. Dyn., 46, 2123-2144, 10.1007/s00382-015-2693-z, 2016.
- 1126 Fang, J.-Y., and Yoda, K.: Climate and vegetation in China (I). Changes in the
1127 altitudinal lapse rate of temperature and distribution of sea level temperature, Ecol.
1128 Res., 3, 37-51, 1988.
- 1129 Fujiwara, M., Wright, J. S., Manney, G. L., Gray, L. J., Anstey, J., Birner, T., Davis, S.,
1130 Gerber, E. P., Harvey, V. L., Hegglin, M. I., Homeyer, C. R., Knox, J. A., Kruger, K.,
1131 Lambert, A., Long, C. S., Martineau, P., Molod, A., Monge-Sanz, B. M., Santee, M.
1132 L., Tegtmeier, S., Chabillat, S., Tan, D. G. H., Jackson, D. R., Polavarapu, S., Compo,
1133 G. P., Dragani, R., Ebisuzaki, W., Harada, Y., Kobayashi, C., McCarty, W., Onogi, K.,
1134 Pawson, S., Simmons, A., Wagan, K., Whitaker, J. S., and Zou, C.-Z.: Introduction to
1135 the SPARC reanalysis intercomparison project (S-RIP) and overview of the reanalysis
1136 systems, Atmos. Chem. Phys., 17, 1417-1452, 10.5194/acp-17-1417-2017, 2017.
- 1137 Gervais, M., Gyakum, J. R., Atallah, E., Tremblay, L. B., and Neale, R. B.: How well
1138 are the distribution and extreme values of daily precipitation over North America
1139 represented in the community climate system model? A comparison to reanalysis,
1140 satellite, and gridded station data, J. Clim., 27, 5219-5239, 10.1175/jcli-d-13-00320.1,
1141 2014.
- 1142 Gibson, J., Källberg P, Uppala S, Nomura A, Hernandez A, and E., S.: ERA
1143 description, ECMWF. ERA-15 Project Report Series 1, European Centre for
1144 Medium-range Weather Forecasts, Reading, UK., 1997.
- 1145 Golub, G. H., and Van Loan, C. F.: An analysis of the total least squares problem,
1146 SIAM J. Numer. Anal., 17, 883-893, 1980.
- 1147 Heng, Z., Fu, Y., Liu, G., Zhou, R., Wang, Y., Yuan, R., Guo, J., and Dong, X.: A
1148 study of the distribution and variability of cloud water using ISCCP, SSM/I cloud
1149 product, and reanalysis datasets, J. Clim., 27, 3114-3128, 10.1175/jcli-d-13-00031.1,
1150 2014.
- 1151 Herring, S. C., Christidis, N., Hoell, A., Kossin, J. P., Schreck III, C., and Stott, P. A.:
1152 Explaining extreme events of 2016 from a climate perspective, Bull. Am. Meteorol.
1153 Soc., 99, S1-S157, 2018.
- 1154 Hersbach, H., Peubey, C., Simmons, A., Berrisford, P., Poli, P., and Dee, D.:

- 1155 ERA-20CM: a twentieth-century atmospheric model ensemble, *Q. J. Roy. Meteorol.*
1156 Soc., 141, 2350-2375, 10.1002/qj.2528, 2015.
- 1157 Hines, K. M., Bromwich, D. H., and Marshall, G. J.: Artificial surface pressure trends
1158 in the NCEP-NCAR reanalysis over the southern ocean and Antarctica, *J. Clim.*, 13,
1159 3940-3952, 10.1175/1520-0442(2000)013<3940:aspit>2.0.co;2, 2000.
- 1160 Hyk, W., and Stojek, Z.: Quantifying uncertainty of determination by standard
1161 additions and serial dilutions methods taking into account standard uncertainties in
1162 both axes, *Anal. Chem.*, 85, 5933-5939, 2013.
- 1163 Kalnay, E., Kanamitsu, M., Kistler, R., Collins, W., Deaven, D., Gandin, L., Iredell,
1164 M., Saha, S., White, G., and Woollen, J.: The NCEP/NCAR 40-year reanalysis project,
1165 *Bull. Am. Meteorol. Soc.*, 77, 437-471, 1996.
- 1166 Kanamitsu, M., Ebisuzaki, W., Woollen, J., Yang, S.-K., Hnilo, J. J., Fiorino, M., and
1167 Potter, G. L.: NCEP–DOE AMIP-II Reanalysis (R-2), *Bull. Am. Meteorol. Soc.*, 83,
1168 1631-1643, 10.1175/BAMS-83-11-1631, 2002.
- 1169 Kidston, J., Frierson, D. M. W., Renwick, J. A., and Vallis, G. K.: Observations,
1170 simulations, and dynamics of jet stream variability and annular modes, *J. Clim.*, 23,
1171 6186-6199, 10.1175/2010jcli3235.1, 2010.
- 1172 Kobayashi, S., Ota, Y., Harada, Y., Ebita, A., Moriya, M., Onoda, H., Onogi, K.,
1173 Kamahori, H., Kobayashi, C., Endo, H., Miyaoka, K., and Takahashi, K.: The JRA-55
1174 reanalysis: general specifications and basic characteristics, *J. Meteorol. Soc. Jpn.*, 93,
1175 5-48, 10.2151/jmsj.2015-001, 2015.
- 1176 Lahoz, W. A., and Schneider, P.: Data assimilation: making sense of Earth
1177 Observation, *Front. Environ. Sci.*, 2, 1-28, 10.3389/fenvs.2014.00016, 2014.
- 1178 Laloyaux, P., Balmaseda, M., Dee, D., Mogensen, K., and Janssen, P.: A coupled data
1179 assimilation system for climate reanalysis, *Q. J. Roy. Meteorol. Soc.*, 142, 65-78,
1180 10.1002/qj.2629, 2016.
- 1181 Li, H. B., Robock, A., Liu, S. X., Mo, X. G., and Viterbo, P.: Evaluation of reanalysis
1182 soil moisture simulations using updated Chinese soil moisture observations, *J.
1183 Hydrometeorol.*, 6, 180-193, 10.1175/jhm416.1, 2005.
- 1184 Li, Q., Zhang, L., Xu, W., Zhou, T., Wang, J., Zhai, P., and Jones, P.: Comparisons of
1185 Time Series of Annual Mean Surface Air Temperature for China since the 1900s:
1186 Observations, Model Simulations, and Extended Reanalysis, *Bull. Am. Meteorol. Soc.*,
1187 98, 699-711, 10.1175/bams-d-16-0092.1, 2017.
- 1188 Li, Y., Zeng, Z. Z., Zhao, L., and Piao, S. L.: Spatial patterns of climatological
1189 temperature lapse rate in mainland China: A multi-time scale investigation, *J Geophys
1190 Res-Atmos.*, 120, 2661-2675, Doi 10.1002/2014jd022978, 2015.

- 1191 Lin, R., Zhou, T., and Qian, Y.: Evaluation of global monsoon precipitation changes
1192 based on five reanalysis datasets, J. Clim., 27, 1271-1289,
1193 doi:10.1175/JCLI-D-13-00215.1, 2014.
- 1194 Lindsay, R., Wensnahan, M., Schweiger, A., and Zhang, J.: Evaluation of seven
1195 different atmospheric reanalysis products in the Arctic, J. Clim., 27, 2588-2606,
1196 10.1175/jcli-d-13-00014.1, 2014.
- 1197 Ma, L., Zhang, T., Li, Q., Frauenfeld, O. W., and Qin, D.: Evaluation of ERA-40,
1198 NCEP-1, and NCEP-2 reanalysis air temperatures with ground-based measurements
1199 in China, J. Geophys. Res. D Atmos., 113, D15115, 10.1029/2007JD009549, 2008.
- 1200 Mao, J., Shi, X., Ma, L., Kaiser, D. P., Li, Q., and Thornton, P. E.: Assessment of
1201 reanalysis daily extreme temperatures with china's homogenized historical dataset
1202 during 1979-2001 using probability density functions, J. Clim., 23, 6605-6623,
1203 10.1175/2010jcli3581.1, 2010.
- 1204 Mitas, C. M., and Clement, A.: Recent behavior of the Hadley cell and tropical
1205 thermodynamics in climate models and reanalyses, Geophys. Res. Lett., 33, L01810,
1206 10.1029/2005gl024406, 2006.
- 1207 Nguyen, H., Evans, A., Lucas, C., Smith, I., and Timbal, B.: The Hadley circulation in
1208 reanalyses: climatology, variability, and change, J. Clim., 26, 3357-3376,
1209 10.1175/jcli-d-12-00224.1, 2013.
- 1210 Niznik, M. J., and Lintner, B. R.: Circulation, moisture, and precipitation relationships
1211 along the south Pacific convergence zone in reanalyses and CMIP5 models, J. Clim.,
1212 26, 10174-10192, 10.1175/jcli-d-13-00263.1, 2013.
- 1213 Onogi, K., Tsltsui, J., Koide, H., Sakamoto, M., Kobayashi, S., Hatsushika, H.,
1214 Matsumoto, T., Yamazaki, N., Kaalhori, H., Takahashi, K., Kadokura, S., Wada, K.,
1215 Kato, K., Oyama, R., Ose, T., Mannaji, N., and Taira, R.: The JRA-25 reanalysis, J.
1216 Meteorol. Soc. Jpn., 85, 369-432, Doi 10.2151/Jmsj.85.369, 2007.
- 1217 Parker, W. S.: Reanalyses and observations: What's the difference?, Bull. Am.
1218 Meteorol. Soc., 97, 1565-1572, 10.1175/bams-d-14-00226.1, 2016.
- 1219 Peña, M., and Toth, Z.: Estimation of analysis and forecast error variances, Tellus A,
1220 66, 21767, 2014.
- 1221 Piao, S. L., Yin, L., Wang, X. H., Ciais, P., Peng, S. S., Shen, Z. H., and Seneviratne,
1222 S. I.: Summer soil moisture regulated by precipitation frequency in China, Environ.
1223 Res. Lett., 4, 044012, 10.1088/1748-9326/4/4/044012, 2009.
- 1224 Pitman, A. J., and Perkins, S. E.: Global and regional comparison of daily 2-m and
1225 1000-hpa maximum and minimum temperatures in three global reanalyses, J. Clim.,
1226 22, 4667-4681, 10.1175/2009jcli2799.1, 2009.

- 1227 Poli, P., Healy, S. B., and Dee, D. P.: Assimilation of Global Positioning System radio
1228 occultation data in the ECMWF ERA-Interim reanalysis, *Q. J. Roy. Meteorol. Soc.*,
1229 136, 1972-1990, 10.1002/qj.722, 2010.
- 1230 Poli, P., Hersbach, H., Dee, D. P., Berrisford, P., Simmons, A. J., Vitart, F., Laloyaux,
1231 P., Tan, D. G. H., Peubey, C., Thépaut, J.-N., Trémolet, Y., Hólm, E. V., Bonavita, M.,
1232 Isaksen, L., and Fisher, M.: ERA-20C: An atmospheric reanalysis of the twentieth
1233 century, *J. Clim.*, 29, 4083-4097, doi:10.1175/JCLI-D-15-0556.1, 2016.
- 1234 Qian, T. T., Dai, A., Trenberth, K. E., and Oleson, K. W.: Simulation of global land
1235 surface conditions from 1948 to 2004. Part I: Forcing data and evaluations, *J.*
1236 *Hydrometeorol.*, 7, 953-975, Doi 10.1175/Jhm540.1, 2006.
- 1237 Reed, B. C.: Linear least - squares fits with errors in both coordinates, *Am. J. Phys.*,
1238 57, 642-646, 1989.
- 1239 Reichle, R. H., Koster, R. D., De Lannoy, G. J. M., Forman, B. A., Liu, Q.,
1240 Mahanama, S. P. P., and Touré A.: Assessment and enhancement of MERRA land
1241 surface hydrology estimates, *J. Clim.*, 24, 6322-6338, 10.1175/JCLI-D-10-05033.1,
1242 2011.
- 1243 Reichle, R. H., Liu, Q., Koster, R. D., Draper, C. S., Mahanama, S. P. P., and Partyka,
1244 G. S.: Land surface precipitation in MERRA-2, *J. Clim.*, 30, 1643-1664,
1245 10.1175/jcli-d-16-0570.1, 2017.
- 1246 Reuten, C., Moore, R. D., and Clarke, G. K. C.: Quantifying differences between 2-m
1247 temperature observations and reanalysis pressure-level temperatures in northwestern
1248 North America, *J. Appl. Meteor. Climatol.*, 50, 916-929, 10.1175/2010jamc2498.1,
1249 2011.
- 1250 Riendecker, M. M., Suarez, M. J., Gelaro, R., Todling, R., Bacmeister, J., Liu, E.,
1251 Bosilovich, M. G., Schubert, S. D., Takacs, L., Kim, G.-K., Bloom, S., Chen, J.,
1252 Collins, D., Conaty, A., da Silva, A., Gu, W., Joiner, J., Koster, R. D., Lucchesi, R.,
1253 Molod, A., Owens, T., Pawson, S., Pégion, P., Redder, C. R., Reichle, R., Robertson, F.
1254 R., Ruddick, A. G., Sienkiewicz, M., and Woollen, J.: MERRA: NASA's Modern-Era
1255 Retrospective Analysis for Research and Applications, *J. Clim.*, 24, 3624-3648,
1256 10.1175/JCLI-D-11-00015.1, 2011.
- 1257 Ryan, T. P.: *Modern regression methods*, John Wiley & Sons, 2008.
- 1258 Saha, S., Moorthi, S., Pan, H. L., Wu, X. R., Wang, J. D., Nadiga, S., Tripp, P., Kistler,
1259 R., Woollen, J., Behringer, D., Liu, H. X., Stokes, D., Grumbine, R., Gayno, G., Wang,
1260 J., Hou, Y. T., Chuang, H. Y., Juang, H. M. H., Sela, J., Iredell, M., Treadon, R., Kleist,
1261 D., Van Delst, P., Keyser, D., Derber, J., Ek, M., Meng, J., Wei, H. L., Yang, R. Q.,
1262 Lord, S., Van den Dool, H., Kumar, A., Wang, W. Q., Long, C., Chelliah, M., Xue, Y.,
1263 Huang, B. Y., Schemm, J. K., Ebisuzaki, W., Lin, R., Xie, P. P., Chen, M. Y., Zhou, S.

- 1264 T., Higgins, W., Zou, C. Z., Liu, Q. H., Chen, Y., Han, Y., Cucurull, L., Reynolds, R.
1265 W., Rutledge, G., and Goldberg, M.: The NCEP climate forecast system reanalysis,
1266 Bull. Am. Meteorol. Soc., 91, 1015-1057, 10.1175/2010BAMS3001.1, 2010.
- 1267 Schoeberl, M. R., Dessler, A. E., and Wang, T.: Simulation of stratospheric water
1268 vapor and trends using three reanalyses, Atmos. Chem. Phys., 12, 6475-6487,
1269 10.5194/acp-12-6475-2012, 2012.
- 1270 Shen, M., Piao, S., Jeong, S.-J., Zhou, L., Zeng, Z., Ciais, P., Chen, D., Huang, M., Jin,
1271 C.-S., and Li, L. Z.: Evaporative cooling over the Tibetan Plateau induced by
1272 vegetation growth, Proc. Nat. Acad. Sci. U.S.A., 112, 9299-9304, 2015.
- 1273 Simmonds, I., and Keay, K.: Mean Southern Hemisphere extratropical cyclone
1274 behavior in the 40-year NCEP-NCAR reanalysis, J. Clim., 13, 873-885,
1275 10.1175/1520-0442(2000)013<0873:mshecb>2.0.co;2, 2000.
- 1276 Simmons, A. J., Willett, K. M., Jones, P. D., Thorne, P. W., and Dee, D. P.:
1277 Low-frequency variations in surface atmospheric humidity, temperature, and
1278 precipitation: Inferences from reanalyses and monthly gridded observational data sets,
1279 J. Geophys. Res. D Atmos., 115, D01110, 10.1029/2009JD012442, 2010.
- 1280 Siswanto, S., Oldenborgh, G. J., Schrier, G., Jilderda, R., and Hurk, B.: Temperature,
1281 extreme precipitation, and diurnal rainfall changes in the urbanized Jakarta city during
1282 the past 130 years, Int. J. Climatol., 36, 3207-3225, 2015.
- 1283 Spracklen, D. V., Arnold, S. R., and Taylor, C. M.: Observations of increased tropical
1284 rainfall preceded by air passage over forests, Nature, 494, 390-390,
1285 10.1038/nature11904, 2013.
- 1286 Stott, P.: How climate change affects extreme weather events, Science, 352,
1287 1517-1518, 10.1126/science.aaf7271, 2016.
- 1288 Tang, W.-J., Yang, K., Qin, J., Cheng, C., and He, J.: Solar radiation trend across
1289 China in recent decades: a revisit with quality-controlled data, Atmos. Chem. Phys.,
1290 11, 393-406, 2011.
- 1291 Tellinghuisen, J.: Least-squares analysis of data with uncertainty in x and y: A Monte
1292 Carlo methods comparison, Chemom. Intell. Lab. Syst., 103, 160-169, 2010.
- 1293 Thorne, P., and Vose, R.: Reanalyses suitable for characterizing long-term trends: Are
1294 they really achievable?, Bull. Am. Meteorol. Soc., 91, 353-361, 2010.
- 1295 Trenberth, K. E., and Olson, J. G.: An evaluation and intercomparison of global
1296 analyses from the National-Meteorological-Center and the
1297 European-Centre-for-Medium-Range-Weather-Forecasts, Bull. Am. Meteorol. Soc.,
1298 69, 1047-1057, Doi 10.1175/1520-0477(1988)069<1047:Aeaiog>2.0.Co;2, 1988.

- 1299 Trenberth, K. E.: Climatology - Rural land-use change and climate, *Nature*, 427,
1300 213-213, 10.1038/427213a, 2004.
- 1301 Trenberth, K. E., Koike, T., and Onogi, K.: Progress and prospects for reanalysis for
1302 weather and climate, *Eos Trans. Am. Geophys. Union*, 89, 234-235,
1303 10.1029/2008EO260002, 2008.
- 1304 Trenberth, K. E., Fasullo, J. T., and Mackaro, J.: Atmospheric Moisture Transports
1305 from Ocean to Land and Global Energy Flows in Reanalyses, *J. Clim.*, 24, 4907-4924,
1306 10.1175/2011JCLI4171.1, 2011.
- 1307 Trenberth, K. E., Fasullo, J. T., and Shepherd, T. G.: Attribution of climate extreme
1308 events, *Nature Clim. Change*, 5, 725-730, 10.1038/nclimate2657, 2015.
- 1309 Trenberth, K. E., and Zhang, Y.: "How often does it really rain?", *Bull. Am. Meteorol.
1310 Soc.*, published online, 10.1175/bams-d-17-0107.1, 2017.
- 1311 Trigo, I., Boussetta, S., Viterbo, P., Balsamo, G., Beljaars, A., and Sandu, I.:
1312 Comparison of model land skin temperature with remotely sensed estimates and
1313 assessment of surface - atmosphere coupling, *J. Geophys. Res. D Atmos.*, 120,
1314 D023812, 10.1002/2015JD023812, 2015.
- 1315 Tsidu, G. M.: High-resolution monthly rainfall database for Ethiopia: Homogenization,
1316 reconstruction, and gridding, *J. Clim.*, 25, 8422-8443, 10.1175/jcli-d-12-00027.1,
1317 2012.
- 1318 Uppala, S. M., Kållberg, P. W., Simmons, A. J., Andrae, U., Bechtold, V. D. C.,
1319 Fiorino, M., Gibson, J. K., Haseler, J., Hernandez, A., Kelly, G. A., Li, X., Onogi, K.,
1320 Saarinen, S., Sokka, N., Allan, R. P., Andersson, E., Arpe, K., Balmaseda, M. A.,
1321 Beljaars, A. C. M., Berg, L. V. D., Bidlot, J., Bormann, N., Caires, S., Chevallier, F.,
1322 Dethof, A., Dragosavac, M., Fisher, M., Fuentes, M., Hagemann, S., Hólm, E.,
1323 Hoskins, B. J., Isaksen, L., Janssen, P. A. E. M., Jenne, R., McNally, A. P., Mahfouf, J.
1324 F., Morcrette, J. J., Rayner, N. A., Saunders, R. W., Simon, P., Sterl, A., Trenberth, K.
1325 E., Untch, A., Vasiljevic, D., Viterbo, P., and Woollen, J.: The ERA-40 re-analysis, Q.
1326 J. Roy. Meteorol. Soc., 131, 2961-3012, 10.1256/qj.04.176, 2005.
- 1327 Venema, V., Mestre, O., Aguilar, E., Auer, I., Guijarro, J., Domonkos, P., Vertacnik, G.,
1328 Szentimrey, T., Stepanek, P., and Zahradnicek, P.: Benchmarking homogenization
1329 algorithms for monthly data, *Clim. Past*, 8, 89-115, 2012.
- 1330 Voosen, P.: GPS satellites yield space weather data, *Science*, 355, 443-443,
1331 10.1126/science.355.6324.443, 2017.
- 1332 Wang, A., and Zeng, X.: Evaluation of multireanalysis products with in situ
1333 observations over the Tibetan Plateau, *J. Geophys. Res. D Atmos.*, 117, D05102,
1334 10.1029/2011JD016553, 2012.

- 1335 Wang, K., and Liang, S.: Global atmospheric downward longwave radiation over land
1336 surface under all - sky conditions from 1973 to 2008, *J. Geophys. Res. D Atmos.*, 114,
1337 D19101, 2009.
- 1338 Wang, K., Dickinson, R., Wild, M., and Liang, S.: Atmospheric impacts on climatic
1339 variability of surface incident solar radiation, *Atmos. Chem. Phys.*, 12, 9581-9592,
1340 2012.
- 1341 Wang, K., and Dickinson, R. E.: Global atmospheric downward longwave radiation at
1342 the surface from ground-based observations, satellite retrievals, and reanalyses, *Rev.
1343 Geophys.*, 51, 150-185, 10.1002/rog.20009, 2013.
- 1344 Wang, K.: Measurement biases explain discrepancies between the observed and
1345 simulated decadal variability of surface incident solar radiation, *Sci. Rep.*, 4, 6144,
1346 10.1038/srep06144, 2014.
- 1347 Wang, K. C., Ma, Q., Li, Z. J., and Wang, J. K.: Decadal variability of surface incident
1348 solar radiation over China: Observations, satellite retrievals, and reanalyses, *J
1349 Geophys Res-Atmos*, 120, 6500-6514, 10.1002/2015JD023420, 2015.
- 1350 Wang, X., and Wang, K.: Homogenized variability of radiosonde-derived atmospheric
1351 boundary layer height over the global land surface from 1973 to 2014, *J. Clim.*, 29,
1352 6893-6908, doi:10.1175/JCLI-D-15-0766.1, 2016.
- 1353 Wang, X. L., Wen, Q. H., and Wu, Y.: Penalized maximal t test for detecting
1354 undocumented mean change in climate data series, *J. Appl. Meteor. Climatol.*, 46,
1355 916-931, 2007.
- 1356 Wang, X. L.: Penalized maximal F test for detecting undocumented mean shift
1357 without trend change, *J. Atmos. Oceanic Technol.*, 25, 368-384, 2008.
- 1358 Wang, X. L., Chen, H., Wu, Y., Feng, Y., and Pu, Q.: New techniques for the detection
1359 and adjustment of shifts in daily precipitation data series, *J. Appl. Meteor. Climatol.*,
1360 49, 2416-2436, 2010.
- 1361 Wang, X. L., and Feng, Y.: RHtestsV4 user manual, Atmospheric Science and
1362 Technology Directorate, Science and Technology Branch, Environment Canada. 28 pp.
1363 available at <http://etccdi.pacificclimate.org/software.shtml>, 2013.
- 1364 Wu, C., Chen, J. M., Pumpanen, J., Cescatti, A., Marcolla, B., Blanken, P. D., Ardö, J.,
1365 Tang, Y., Magliulo, V., and Georgiadis, T.: An underestimated role of precipitation
1366 frequency in regulating summer soil moisture, *Environ. Res. Lett.*, 7, 024011, 2012.
- 1367 Xu, J., and Powell, A. M., Jr.: Uncertainty of the stratospheric/tropospheric
1368 temperature trends in 1979-2008: multiple satellite MSU, radiosonde, and reanalysis
1369 datasets, *Atmos. Chem. Phys.*, 11, 10727-10732, 10.5194/acp-11-10727-2011, 2011.

- 1370 Yang, K., Koike, T., and Ye, B.: Improving estimation of hourly, daily, and monthly
1371 solar radiation by importing global data sets, *Agr. Forest Meteorol.*, 137, 43-55,
1372 10.1016/j.agrformet.2006.02.001, 2006.
- 1373 York, D., Evensen, N. M., Martínez, M. L., and Delgado, J. D. B.: Unified equations
1374 for the slope, intercept, and standard errors of the best straight line, *Am. J. Phys.*, 72,
1375 367-375, 10.1119/1.1632486, 2004.
- 1376 You, Q., Kang, S., Pepin, N., Flügel, W.-A., Yan, Y., Behravan, H., and Huang, J.:
1377 Relationship between temperature trend magnitude, elevation and mean temperature
1378 in the Tibetan Plateau from homogenized surface stations and reanalysis data, *Global*
1379 *Planet. Change*, 71, 124-133, 10.1016/j.gloplacha.2010.01.020, 2010.
- 1380 Zeng, Z., Piao, S., Li, L. Z., Zhou, L., Ciais, P., Wang, T., Li, Y., Lian, X., Wood, E. F.,
1381 and Friedlingstein, P.: Climate mitigation from vegetation biophysical feedbacks
1382 during the past three decades, *Nature Clim. Change*, 7, 432-436, 2017.
- 1383 Zhao, T., Guo, W., and Fu, C.: Calibrating and evaluating reanalysis surface
1384 temperature error by topographic correction, *J. Clim.*, 21, 1440-1446,
1385 10.1175/2007jcli1463.1, 2008.
- 1386 Zhou, C., and Wang, K.: Evaluation of surface fluxes in ERA-Interim using flux
1387 tower data, *J. Clim.*, 29, 1573-1582, 10.1175/JCLI-D-15-0523.1, 2016a.
- 1388 Zhou, C., and Wang, K.: Biological and environmental controls on evaporative
1389 fractions at ameriflux sites, *J. Appl. Meteor. Climatol.*, 55, 145-161,
1390 10.1175/JAMC-D-15-0126.1, 2016b.
- 1391 Zhou, C., and Wang, K.: Spatiotemporal divergence of the warming hiatus over land
1392 based on different definitions of mean temperature, *Sci. Rep.*, 6, 31789,
1393 10.1038/srep31789, 2016c.
- 1394 Zhou, C., and Wang, K.: Land surface temperature over global deserts: means,
1395 variability and trends, *J. Geophys. Res. D Atmos.*, 121, 2016JD025410,
1396 10.1002/2016JD025410, 2016d.
- 1397 Zhou, C., and Wang, K.: Contrasting daytime and nighttime precipitation variability
1398 between observations and eight reanalysis products from 1979 to 2014 in China, *J.*
1399 *Clim.*, 30, 6443-6464, 10.1175/JCLI-D-16-0702.1, 2017a.
- 1400 Zhou, C., and Wang, K.: Quantifying the sensitivity of precipitation to the long-term
1401 warming trend and interannual-decadal variation of surface air temperature over
1402 China, *J. Clim.*, 30, 3687-3703, 10.1175/jcli-d-16-0515.1, 2017b.
- 1403 Zhou, C., Wang, K., and Ma, Q.: Evaluation of eight current reanalyses in simulating
1404 land surface temperature from 1979 to 2003 in China, *J. Clim.*, 30, 7379-7398,
1405 10.1175/jcli-d-16-0903.1, 2017.

1406 Zhou, C., Wang, K., and Qi, D.: Attribution of the July 2016 extreme precipitation
1407 event over China's Wuhan, Bull. Am. Meteorol. Soc., 99, S107-S112, 2018.

1408

1409

1410 **Table 1.** Summarized information on the twelve reanalysis twelve products, including
 1411 institution, model resolution, assimilation system, included surface observations included associated with surface air
 1412 temperatures, sea ice and sea surface temperatures SST (SSTsea surface temperature) and GHGs greenhouse gas (GHG)
 1413 boundary conditions. The number in the parentheses of Column in the Model Name column is the year for of the
 1414 version of the forecast model used. More details for on each product can be found in the associated reference.

Reanalysis	Institution	Model Name	Model Resolution	Period	Assimilation System
ERA-Interim	ECMWF	IFS version Cy31r2 (2007)	T255 ~80 km, 60 levels	1979 onwards	4D-VAR
JRA-55	JMA	JMA operational numerical weather prediction system (2009)	T319 ~55 km, 60 levels	1958-2013	4D-VAR
NCEP-R1	NCEP/NCAR	NCEP operational numerical weather prediction system (1995)	T62 ~210 km, 28 levels	1948 onwards	3D-VAR
NCEP-R2	NCEP/DOE	Modified NCEP-R1 model (1998)	T62 ~210 km, 28 levels	1979 onwards	3D-VAR
MERRA	NASA/GMAO	An GEOS-5.0.2 atmospheric general circulation model (2008)	0.5 °x0.667 ° ~55 km, 72 levels	1979 onwards	3D-VAR with incremental updating (GEOS IAU)
MERRA-2	NASA/GMAO	The updated version model of GEOS-5.12.4 as used in MERRA; and its land version model is similar to that of MERRA-land (2015)	0.5 °x0.625 ° ~55 km, 72 levels	1980 onwards	3D-VAR with incremental updating (GEOS IAU)
ERA-20C	ECMWF	IFS version Cy38r1 (2012), coupled atmosphere-land-ocean-waves system	T159 ~125 km, 91 levels	1900-2010	4D-VAR
ERA-20CM	ECMWF	The similar model as to that used in ERA-20C (2012)	T159 ~125 km, 91 levels	1900-2010	3D-VAR
CERA-20C	ECMWF	IFS version Cy41r2 (2016), coupled atmosphere-ocean-land-waves-sea ice system	T159 ~125 km, 91 levels	1901-2010	CERA ensemble assimilation technique
NOAA 20CRv2c	NOAA/ESRL PSD	NCEP GFS (2008), an updated version of the NCEP's CFS, Climate Forecast System (CFS) coupled atmosphere-land model	T62 ~210 km, 28 levels	1851-2014	Ensemble Kalman Filter
NOAA 20CRv2	NOAA/ESRL PSD	The same model as NOAA 20CRv2c (2008)	T62 ~210 km, 28 levels	1871-2012	Ensemble Kalman Filter
CFSR	NCEP	NCEP Climate Forecast System (CFS) (2011), coupled atmosphere-ocean-land-sea ice model	T382 ~38 km, 64 levels	1979-2010	3D-VAR

1415 | Table 1. Continued at from right column.

Related Assimilated and /analyzed Analysed Observations	Sea Ice and SSTs	GHGs-Forcing	Reference
1) Includes <i>in-situ</i> observations of near-surface air temperature/pressure/relative humidity 2) Assimilate upper-air temperatures/wind/specific humidity 3) Assimilate rain-affected SSM/I radiances	A changing suite of SST and sea ice data from the observations and the NCEP	Interpolation by 1.6 ppm/year from the global mean CO ₂ in 1990 of 353 ppmv of global mean CO ₂ in 1990	(Dee et al., 2011b)
1) Analyzed Analyses available near-surface observations 2) Assimilate all available traditional and satellite observations	In-situ In-situ observation-based estimates of the COBE SST data and sea ice	The same as CMIP5 Same as CMIP5	(Kobayashi et al., 2015)
1) Initiated with weather observations from ships, planes, station data, satellite observations and many more sources 2) No inclusion of near-surface air temperatures 3) Use observed precipitation to nudge soil moisture 4) No information on aerosols	Reynolds SSTs for 1982 on and the UKMO GISST data for earlier periods	Constant global mean CO ₂ of 330 ppmv and no other ppmv; no other trace gases	(Kalnay et al., 1996)
1) No inclusion of near-surface air temperature 2) No information on aerosols	AMIP-II prescribed	Constant global mean CO ₂ , 350 ppmv and no other ppmv; no other trace gases	(Kanamitsu et al., 2002)
1) Neither MERRA nor MERRA-2 analyzed analyse near-surface air temperature, relative humidity and so on, or other variables 2) The Radiosondes do provide some low-level observations	Reynolds SSTs prescribed	The same as CMIP5 Same as CMIP5	(Rienecker et al., 2011)
1) Includes newer observations (not included in MERRA) after the 2010s 2) Includes aerosols from MODIS and AERONET measurements over land after the 2000s and from the GOCART model before the 2000s 3) Assimilate observation-corrected precipitation to correct the model-generated precipitation before reaching the land surface	AMIP-II and Reynolds SSTs	The same as CMIP5 Same as CMIP5	(Reichle et al., 2017)
1) Assimilate surface pressures from ISPDv3.2.6 and ICOADSv2.5.1, and surface marine winds from ICOADSv2.5.1 2) Use monthly climatology of aerosols from CMIP5	SST/sea-ice SSTs and sea ice from HadISST2.1.0.0	The same as CMIP5 Same as CMIP5	(Poli et al., 2016)
Assimilate no data and includes radiative forcings from CMIP5	SST/sea-ice SSTs and sea ice realizations from HadISST2.1.0.0 used in 10 members	The same as CMIP5 Same as CMIP5	(Hersbach et al., 2015)
1) Assimilate surface pressures from ISPDv3.2.6 and ICOADSv2.5.1, and surface marine winds from ICOADSv2.5.1 2) Assimilate no data in the land, wave and sea-ice components, but use the coupled model at each time step	SSTs from the HadISST2.1.0.0	The same as CMIP5 Same as CMIP5	(Laloyaux et al., 2016)
Assimilate only surface pressure and sea level pressure	SSTs from HadISST1.1 and sea ice from the COBE SST-SST	Monthly 15° gridded estimation estimates of CO ₂ -CO ₂ from WMO observations	(Compo et al., 2011)
The same Same as NOAA 20CRv2c	SST/sea-ice SSTs and sea ice from HadISST1.1	Monthly 15° gridded estimation estimates of CO ₂ -CO ₂ from WMO observations	(Compo et al., 2011)
1) Assimilate all available conventional and satellite observations, but not near-surface air temperatures 2) Atmospheric model contains observed changes in aerosols 3) Use observation-corrected precipitation to force the land surface analysis	Generated by coupled ocean-sea ice models evolving, evolves freely during the 6-h coupled model integration	Monthly 15° gridded estimation estimates of CO ₂ -CO ₂ from WMO observations	(Saha et al., 2010)

1416

1417 **Table 2.** Differences (unit: °C) relative to the homogeneous homogenized observations and Trends (unit: °C/decade) in
 1418 surface air temperatures (T_a) from 1979 to 2010 over China and its seven subregions. The bold and italic bold fonts
 1419 indicate results that are significant according to a two-tailed Student's t-tests with a significance levels of 0.05 and 0.1,
 1420 respectively.

Regions	China		Tibetan Plateau		Northwest China		Loess Plateau		Middle China		Northeast China		North China		Southeast China	
	Diff.	Trend	Diff.	Trend	Diff.	Trend	Diff.	Trend	Diff.	Trend	Diff.	Trend	Diff.	Trend	Diff.	Trend
ERA-Interim	-0.87	0.38	-3.49	0.33	-1.82	0.37	-0.32	0.50	-1.19	0.28	-0.03	0.42	-0.02	0.45	-0.03	0.37
NCEP-R1	-2.56	0.23	-6.80	0.11	-4.45	0.39	-1.77	0.21	-2.91	0.23	-1.28	0.27	-1.21	0.23	-1.33	0.22
MERRA	-0.48	0.25	-3.48	0.33	0.95	0.14	1.14	0.09	-1.35	0.12	-0.22	0.52	0.67	0.26	-0.27	0.24
JRA-55	-1.10	0.38	-3.49	0.42	-1.70	0.39	-0.58	0.52	-1.61	0.30	-0.25	0.37	-0.26	0.41	-0.50	0.34
NCEP-R2	-2.10	0.25	-5.76	-0.07	-4.29	0.58	-1.33	0.10	-2.80	0.20	-0.51	0.36	-0.38	0.23	-1.14	0.36
MERRA2	-0.91	0.28	-3.41	0.35	0.34	0.32	0.12	0.19	-1.35	0.23	-0.73	0.41	-0.24	0.18	-0.64	0.25
ERA-20C	-1.42	0.29	-6.56	0.33	-1.95	0.31	0.03	0.21	-2.01	0.35	-0.19	0.32	1.05	0.19	-0.47	0.28
ERA-20CM	-1.48	0.32	-5.93	0.28	-1.39	0.38	-0.36	0.33	-2.13	0.27	-0.23	0.41	-0.31	0.34	-0.51	0.29
CERA-20C	-2.06	0.34	-7.00	0.41	-2.15	0.38	-0.78	0.36	-2.59	0.34	-0.76	0.43	-0.40	0.19	-1.20	0.29
NOAA 20CRv2c	-0.28	0.22	-2.75	0.39	-0.01	0.28	1.62	0.16	-1.68	0.18	-0.16	0.11	1.06	0.15	0.18	0.22
NOAA 20CRv2	-0.32	0.24	-2.78	0.33	-0.01	0.29	1.48	0.20	-1.77	0.19	-0.07	0.25	0.97	0.21	0.12	0.19
CFSR	-1.74	0.48	-5.09	0.46	-1.03	0.44	-0.25	0.40	-2.91	0.37	-0.49	0.67	-0.37	0.47	-1.58	0.51
Obs-raw	0.03	0.40	0.03	0.46	0.09	0.44	0.01	0.52	0.05	0.30	0.00	0.40	0.05	0.42	0.03	0.36
Obs-homogenized		0.37		0.44		0.36		0.50		0.24		0.41		0.38		0.33

1422 **Table 3.** Spatial pattern correlation (unit: 1) of three groups: partial relationships, trends and simulated trend biases of biases in
 1423 the trends in surface air temperature (T_a) against surface incident solar radiation (R_s), precipitation frequency, the frequency of
 1424 precipitation, precipitation frequency (PF) and surface downward longwave radiation (L_d). The bold and italic bold fonts indicate
 1425 a two-tailed Student's t test with a significance level of 0.05 and 0.1, respectively. The bold and italic bold fonts indicate results
 1426 that are significant according to two-tailed Student's t-tests with significance levels of 0.05 and 0.1, respectively.

Pattern Correlation	Partial Relationship						Trend			Trend Bias			
	(T_a, R_s)		(T_a, PF)		(T_a, L_d)		(T_a, T_a)	(T_a, R_s)	(T_a, PF)	(T_a, L_d)	(T_a, R_s)	(T_a, PF)	(T_a, L_d)
	Corr.	Slope	Corr.	Slope	Corr.	Slope							
ERA-Interim	0.29	0.01	0.03	0.31	0.21	0.25	0.47	-0.11	-0.04	0.33	0.26	-0.12	0.10
NCEP-R1	0.30	0.06	0.18	0.30	0.36	0.00	0.02	-0.36	-0.02	0.62	-0.03	-0.04	0.43
MERRA	0.29	0.06	0.13	0.39	0.05	0.20	0.21	0.66	-0.81	-0.53	0.42	-0.62	-0.05
JRA-55	0.35	0.21	0.22	0.16	0.29	0.27	0.54	-0.33	0.31	0.57	0.00	0.14	0.29
NCEP-R2	0.22	0.03	0.20	0.36	0.27	0.04	-0.08	0.18	-0.29	0.28	0.15	-0.14	0.35
MERRA2	0.13	0.05	0.26	0.43	0.09	0.30	0.22	0.30	-0.11	0.11	-0.02	-0.12	0.28
ERA-20C	0.28	-0.07	-0.07	0.43	0.19	0.02	-0.07	0.18	-0.33	0.03	0.11	-0.25	0.31
ERA-20CM	0.24	-0.04	-0.03	0.32	0.26	0.18	0.28	-0.32	0.31	0.83	-0.02	0.12	0.34
CERA-20C	0.41	0.17	0.10	0.37	0.08	0.07	0.29	0.50	-0.58	-0.07	-0.01	-0.22	0.23
NOAA 20CRv2c	0.39	0.15	-0.22	0.25	0.14	0.15	0.08	-0.07	-0.11	0.55	-0.25	-0.05	0.50
NOAA 20CRv2	0.38	0.15	-0.21	0.18	0.14	0.23	0.19	-0.02	-0.20	0.56	-0.18	0.11	0.47
CFSR	0.33	0.12	0.10	0.19	0.37	0.21	0.19	0.11	-0.26	0.07	0.31	-0.08	0.15
Obs-raw								-0.07	0.27	0.50			
Obs-homogenized								-0.09	0.35	0.32			

1427 **Figure Captions:**

1428 **Figure 1.** The multiyear-averaged differences in surface air temperature s (T_a , unit: °C)
1429 during the ~~period of 19~~79-2010 from the ~~twelve reanalysis~~^{twelve}
1430 ~~product~~^{reanalysis products} relative to the ~~homogeneous observation~~^{homogenized}
1431 ~~observations~~ over China, i.e., ~~The reanalysis products are~~ (a) ERA-Interim, (b)
1432 NCEP-R1, (c) MERRA, (d) JRA-55, (e) NCEP-R2, (f) MERRA2, (g) ERA-20C, (h)
1433 ERA-20CM, (i) CERA-20C, (j) NOAA 20CRv2c, (k) NOAA 20CRv2 and (l) CFSR.

1434 The mainland of China is divided into seven regions (~~seen shown~~ in Fig. 1c),
1435 specifically: ① ~~the~~ Tibetan Plateau, ② Northwest China, ③ ~~the~~ Loess Plateau, ④
1436 Middle China, ⑤ Northeast China, ⑥ ~~the~~ North China Plain and ⑦ South China.

1437 **Figure 2.** The impact of ~~inconsistency inconsistencies~~ between station and model
1438 elevations on the simulated multiyear-averaged differences in surface air temperature s
1439 (T_a , unit: °C) during the study ~~period of 19~~79-2010 over China. The
1440 elevation difference (Δ Height) between ~~the~~ stations and ~~the~~ models consists of the
1441 filtering error in ~~the elevations used in the~~ spectral model-elevations (Δf) and ~~the~~
1442 difference in site-to-grid elevations (Δs) due to ~~complex orography the complexity of~~
1443 ~~orographic topography~~. ~~The~~ Δf is derived from the model elevations minus the ‘true’
1444 elevations ~~at in~~ the ~~same model grid~~^{corresponding model grid cells} from GTOPO30.
1445 The GTOPO30 orography is widely used in ~~the~~ reanalyses, e.g., by ECMWF. The
1446 ~~color~~^{colour} bar denotes the station elevations s (unit: m). The relationship of the T_a
1447 differences s is regressed on Δ Height (~~shown in at~~ the bottom of each subfigure) or Δf
1448 and Δs (~~shown in at~~ the top of each subfigure) ~~with~~; ~~the~~ corresponding explained

1449 variances are shown.

1450 **Figure 3.** Taylor diagrams for annual time series of the observed and
1451 reanalyzed analysed surface air temperature anomalies (T_a , unit: °C) from 1979 to
1452 2010 in (a) China and (b-h) the seven subregions. The correlation coefficient,
1453 standard deviation and root mean square error (RMSE) were
1454 calculated against the observed homogeneous homogenized T_a anomalies.

1455 **Figure 4.** Composite map of partial correlation coefficients of the detrended surface
1456 air temperature (T_a , unit: °C) against surface incident solar radiation (R_s), the
1457 precipitation frequency the frequency of precipitation precipitation frequency (PF) and
1458 surface downward longwave radiation (L_d) during the period 1979-2010
1459 from observations and the twelve reanalysis twelve product reanalysis products. The
1460 marker '+' denotes the negative partial correlations of T_a with R_s over the Tibetan
1461 Plateau for in NCEP-R2, ERA-20C and ERA-20CM.

1462 **Figure 5. (a, b)** The observed trends in surface air temperature (T_a , unit: °C/decade)
1463 and the simulated trend biases in biases in the trends in T_a (unit: °C/decade) during the
1464 period 1979-2010 from (c) raw observations and (d-o) the twelve
1465 reanalysis twelve product reanalysis products over China with respect to the
1466 homogeneous observation homogenized observations. The squares denote from the
1467 original homogeneous time series, and the dots denote from the adjusted
1468 homogeneous time series. The probability distribution functions of all of the biases in
1469 the trend biases are shown as colored coloured histograms, and the black stairs are
1470 integrated from the trend biases with a significance level of 0.05 (based on two-tailed

1471 Student's *t*-tests). The cyan ~~and~~ green stars in (k-n) ~~are estimated~~represent estimates
1472 ~~of the trend biases~~biases in the trends outside the ensemble ranges whose locations ~~is~~
1473 ~~are denoted~~ds-in by the black dots shown in (k-n).

1474 **Figure 6.** Composite map of the contributions~~s~~ (unit: °C/decade) of ~~the trend biases~~
1475 ~~in~~biases in the trends in three relevant parameters~~s~~, surface incident solar radiation
1476 (R_s , in red), surface downward longwave radiation (L_d , in green) and ~~the precipitation~~
1477 ~~frequency~~the frequency of precipitation~~precipitation frequency~~ (in blue) to ~~the trend~~
1478 ~~biases in~~biases in the trends in surface air temperature (T_a) during the study ~~period~~
1479 ~~19~~period of 1979-2010 ~~from~~, as estimated using the twelve reanalysis~~s~~
1480 ~~product~~reanalysis products over China.

1481 **Figure 7.** Contribution ~~s~~(unit: °C/decade) of ~~the trend biases in~~biases in the trends in
1482 surface air temperature~~s~~ (T_a) from three relevant parameters, i.e., surface incident
1483 solar radiation (R_s , in brown), surface downward longwave radiation (L_d , in light blue)
1484 and ~~the precipitation frequency~~the frequency of precipitation~~precipitation frequency~~
1485 (PF, in deep blue) during the study ~~period~~1979-2010 from the twelve
1486 reanalysis~~s~~product over China and its seven subregions.

1487 **Figure 8.** Spatial associations of the simulated ~~trend biases in~~biases in the trend in
1488 surface air temperature (T_a) versus ~~relevant~~ three relevant parameters among the
1489 twelve reanalysis~~s~~product over China and its seven subregions (solid lines ~~for~~indicate the
1490 NWP-like reanalyses, and dashed lines ~~for~~indicate the climate reanalyses). The
1491 probability density functions (unit: %) of these ~~trend biases~~biases in the trends
1492 ~~were~~are estimated from approximately 700 $1^\circ \times 1^\circ$ grids~~s~~ grid cells over that cover

1493 China. ~~Median~~ The median values (~~colored~~ coloured dots with error bars of spatial
1494 standard deviations) of ~~the trend biases in~~ biases in the trends in T_a (unit: °C/decade)
1495 in the twelve reanalyses ~~were~~ are regressed onto those of (a) the surface incident solar
1496 radiation (R_s , unit: W m^{-2} /decade), (b) ~~precipitation frequency~~ the frequency of
1497 ~~precipitation~~ precipitation frequency (unit: days/decade) and (c) the surface downward
1498 longwave radiation (L_d , unit: W m^{-2} /decade), using the ordinary least squares method
1499 (OLS, denoted by ~~the~~ dashed grey lines) and the weighted total least squares method
1500 (WTLS, denoted by the solid black lines). The 5–95% confidence intervals of the
1501 regressed slopes obtained by the use of using WTLS ~~were~~ are shown as shading. The
1502 regressed correlations and slopes ~~were~~ are shown as ~~as~~ grey and black ~~font~~ text,
1503 respectively.

NWP-like reanalysis

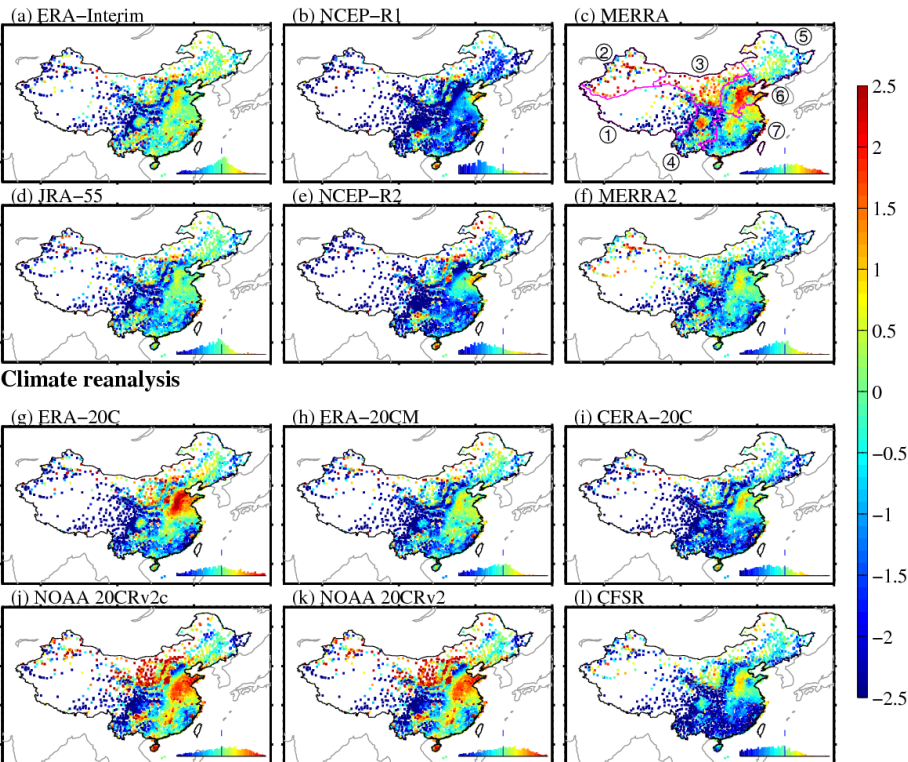


Figure 1. The multiyear-averaged differences in surface air temperature_s (T_a , unit: °C)

1505 during the ~~period 1979-2010~~ from the ~~twelve reanalysis~~¹⁵⁰⁶

~~product~~¹⁵⁰⁷ ~~reanalysis product~~¹⁵⁰⁸ relative to the ~~homogeneous observation~~¹⁵⁰⁹

~~observations~~¹⁵¹⁰ over China, i.e., ~~The reanalysis products are~~¹⁵¹¹ (a) ERA-Interim,

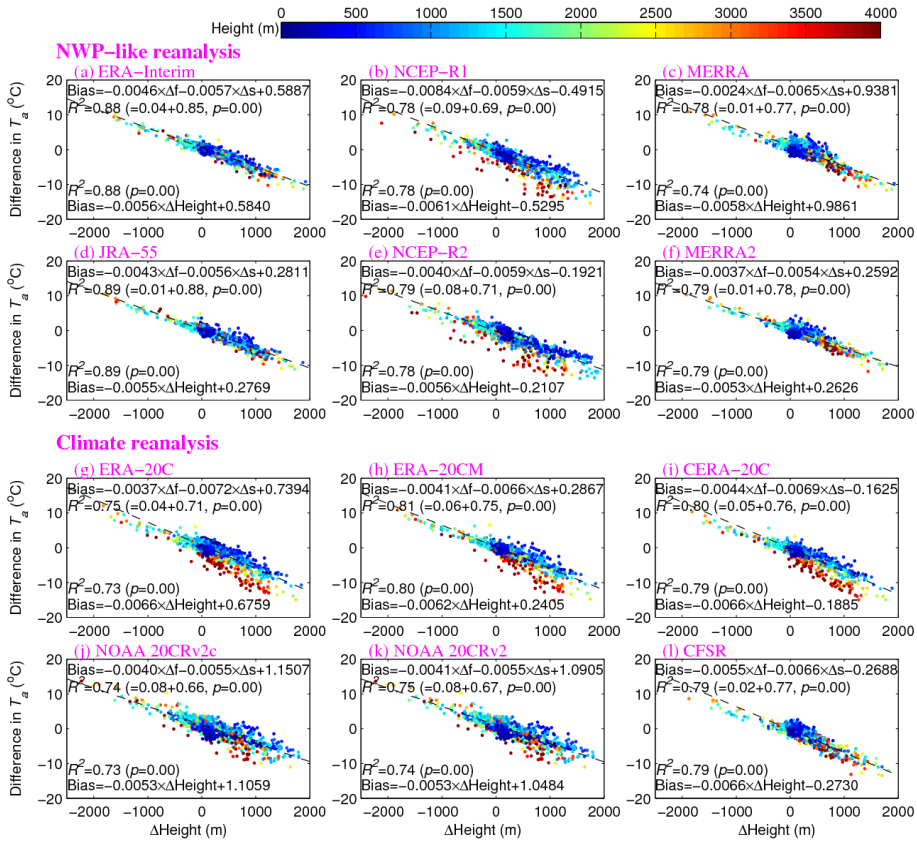
(b) NCEP-R1, (c) MERRA, (d) JRA-55, (e) NCEP-R2, (f) MERRA2, (g) ERA-20C, (h)

(i) ERA-20CM, (j) NOAA 20CRv2c, (k) NOAA 20CRv2 and (l) CFSR.

1512 The mainland of China is divided into seven regions (~~seen shown~~¹⁵¹³ in Fig. 1c),

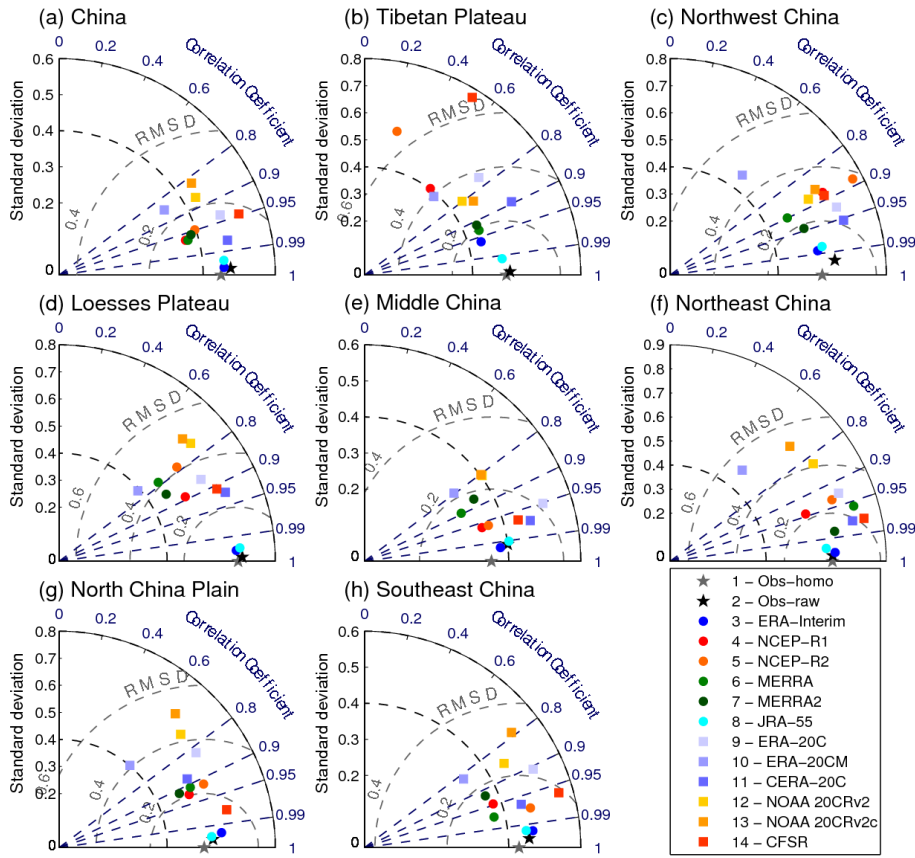
~~specifically~~¹⁵¹⁴ –① ~~the~~ Tibetan Plateau, ② Northwest China, ③ ~~the~~ Loess Plateau, ④

Middle China, ⑤ Northeast China, ⑥ ~~the~~ North China Plain and ⑦ South China.



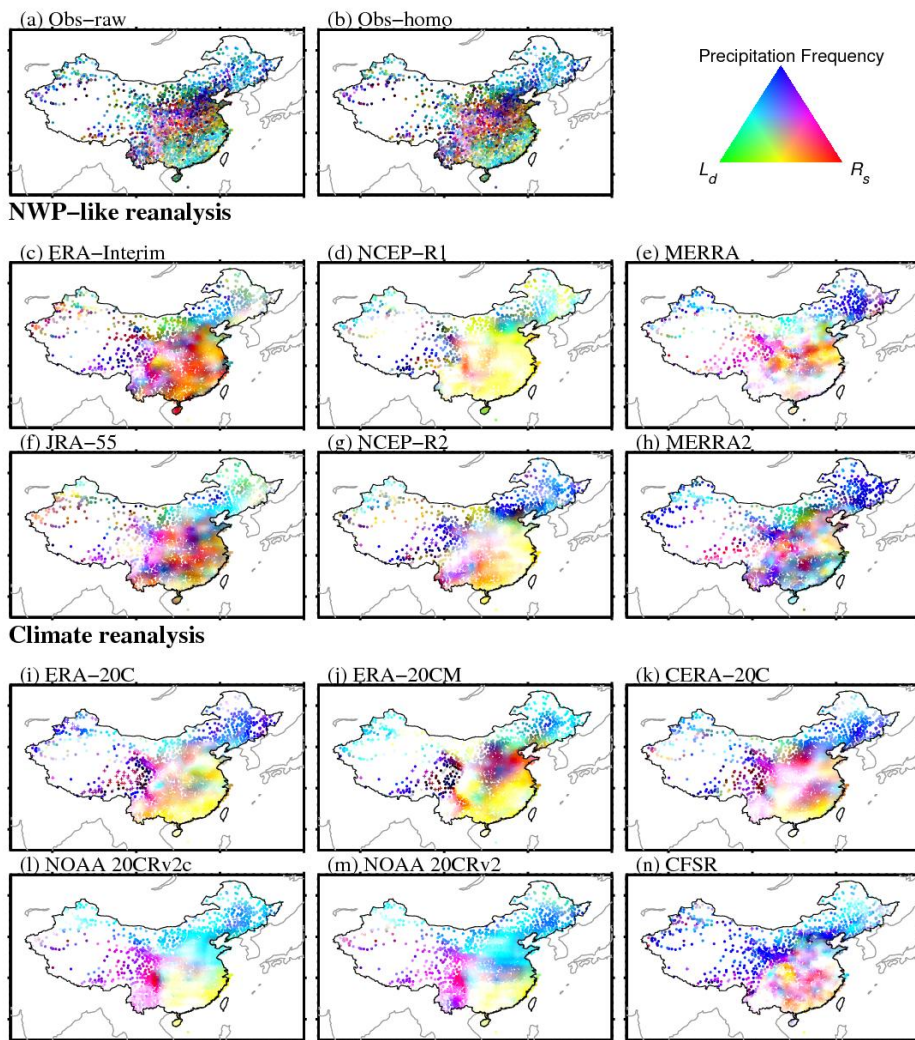
1514
1515 **Figure 2.** The impact of inconsistency inconsistencies between station and model
1516 elevations on the simulated multiyear-averaged differences in surface air temperature~~s~~
1517 (Ta, unit: °C) during the study ~~period~~ ~~19~~ period of 1979-2010 over China. The
1518 elevation difference (ΔHeight) between the stations and the models consists of the
1519 filtering error in the elevations used in the spectral model-elevations (Δf) and the
1520 difference in site-to-grid elevations~~s~~ (Δs) due to ~~complex orography~~ the complexity of
1521 orographic topography. The Δf is derived from the model elevations~~s~~ minus the ‘true’
1522 elevations at in the same model grid corresponding model grid cells from GTOPO30.
1523 The GTOPO30 orography is widely used in the-reanalyses, e.g., by ECMWF. The
1524 color colour bar denotes the station elevations~~s~~ (unit: m). The relationship of the Ta

1525 difference~~s~~ is regressed on Δ Height (shown in-at the bottom of each subfigure) or Δ f
1526 and Δ s (shown in-at the top of each subfigure)-~~with; the~~ corresponding explained
1527 variancesare shown.



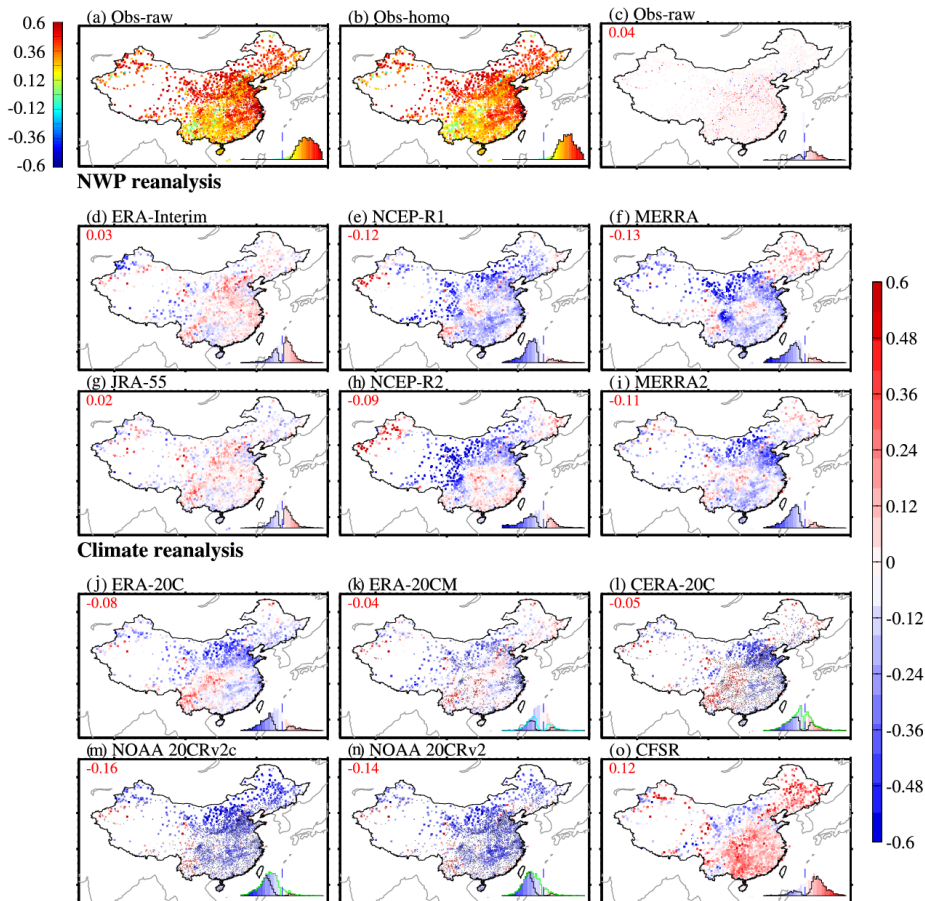
1528

1529 **Figure 3.** Taylor diagrams for annual time series of the observed and
 1530 ~~reanalyzed~~analysed surface air temperature anomalies (T_a , unit: $^{\circ}\text{C}$) from 1979 to
 1531 2010 in (a) China and (b-h) ~~the~~ seven subregions. The correlation coefficient,
 1532 standard deviation and ~~root-mean-square-root mean squared~~ error (RMSE) ~~were are~~
 1533 calculated against the observed ~~homogeneous-homogenized~~ T_a anomalies~~s~~.



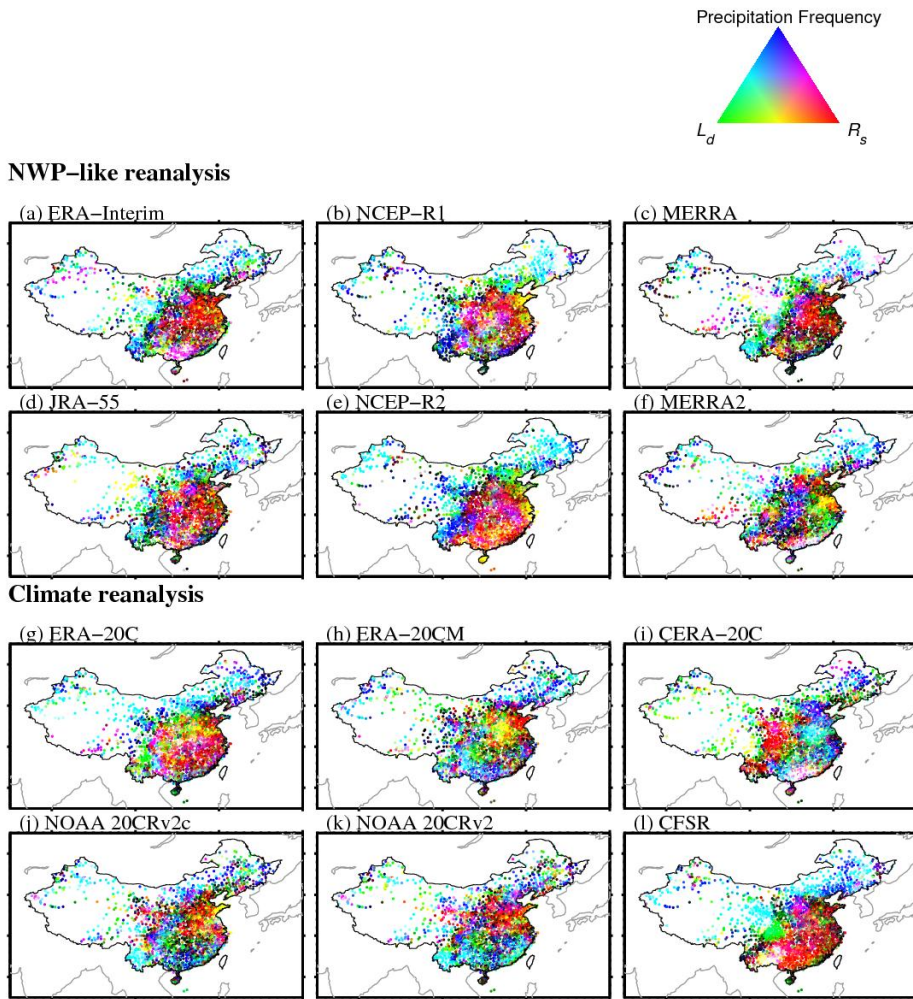
1534

1535 **Figure 4.** Composite map of partial correlation coefficients of the detrended surface
 1536 air temperature (T_a , unit: $^{\circ}\text{C}$) against surface incident solar radiation (R_s), ~~the~~
 1537 ~~precipitation frequency~~~~the frequency of precipitation~~precipitation frequency (PF) and
 1538 surface downward longwave radiation (L_d) during the ~~period 19~~period of 1979-2010
 1539 from observations and the ~~twelve reanalysis~~twelve ~~product~~reanalysis products. The
 1540 marker ‘+’ denotes ~~the~~ negative partial correlations of T_a with R_s over the Tibetan
 1541 Plateau ~~for in~~ NCEP-R2, ERA-20C and ERA-20CM.



1542
 1543 **Figure 5.** (a, b) The observed trends in surface air temperature (T_a , unit: $^{\circ}\text{C}/\text{decade}$)
 1544 and the simulated trend biases in biases in the trends in T_a (unit: $^{\circ}\text{C}/\text{decade}$) during the
 1545 period 1979-2010 from (c) raw observations and (d-o) the twelve
 1546 reanalyses twelve reanalysis products over China with respect to the
 1547 homogenous observation homogenized observations. The squares denote from the
 1548 original homogeneous time series, and the dots denotes from the adjusted
 1549 homogeneous time series. The probability distribution functions of all of the biases in
 1550 the trend biases are shown as colored histograms, and the black stairs are
 1551 integrated from the trend biases with a significance level of 0.05 (based on two-tailed

1552 Student's *t*-tests). The cyan ~~and~~^{green} stars in (k-n) ~~are estimated~~^{represent} estimates
1553 ~~of the trend biases~~^{biases in the trends} outside the ensemble ranges whose locations ~~is~~
1554 ~~are denoted~~^{in by} the black dots ~~shown~~ in (k-n).



1555
1556 **Figure 6.** Composite map of the contributions (unit: $^{\circ}\text{C}/\text{decade}$) of the trend biases
1557 inbiases in the trends in three relevant parameters + surface incident solar radiation
1558 (R_s, in red), surface downward longwave radiation (L_d, in green) and the precipitation
1559 frequencythe frequency of precipitationprecipitation frequency (in blue) to the trend
1560 biases inbiases in the trends in surface air temperature (T_a) during the study period
1561 +19period of 1979-2010 from, as estimated using the twelve reanalysestwelve
1562 productreanalysis products over China.

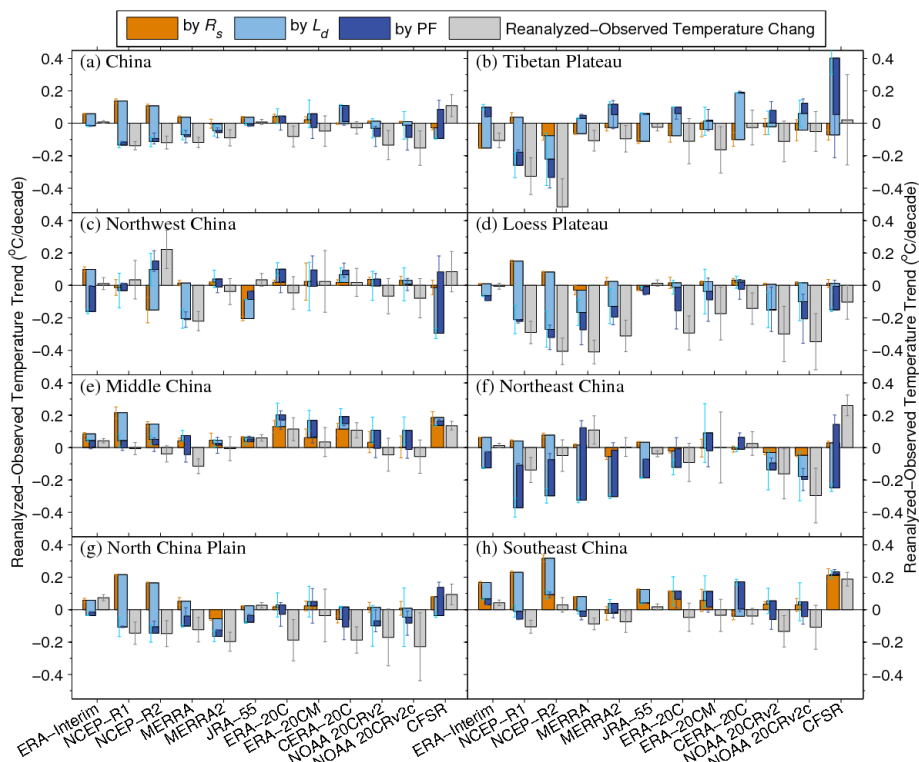
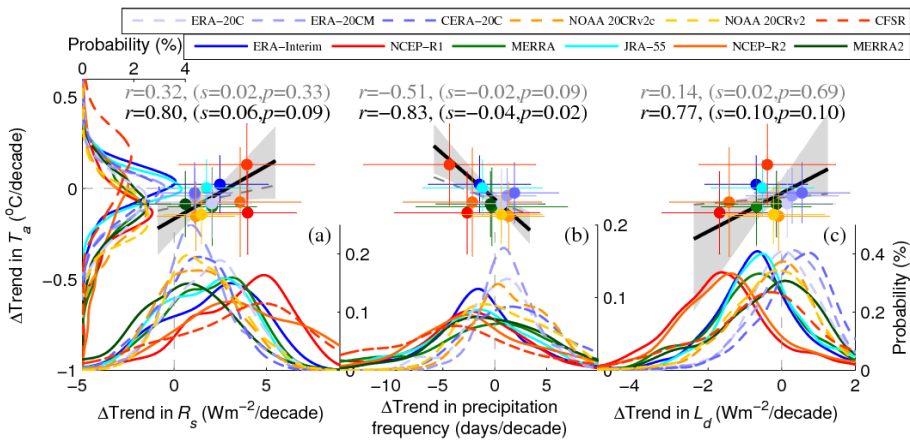


Figure 7. Contribution (unit: $^{\circ}\text{C}/\text{decade}$) of ~~the trend biases in~~ biases in the trends in surface air temperature (T_a) from three relevant parameters, i.e., ~~the~~ surface incident solar radiation (R_s , in brown), surface downward longwave radiation (L_d , in light blue) and ~~the precipitation frequency~~ ~~the frequency of precipitation~~ precipitation frequency (PF, in deep blue) during the study period 1979-2010 from the ~~twelve reanalysis~~ ~~twelve products~~ over China and ~~its~~ seven subregions.



1570

1571 **Figure 8.** Spatial associations of the simulated ~~trend biases in~~ biases in the trend in
 1572 surface air temperature (T_a) versus ~~relevant~~ three relevant parameters among the
 1573 ~~twelve reanalysis~~~~twelve~~ reanalysis products (solid lines ~~for~~ indicate the
 1574 NWP-like reanalyses, and dashed lines ~~for~~ indicate the climate reanalyses). The
 1575 probability density functions (unit: %) of these ~~trend biases~~~~biases in the trends~~
 1576 ~~were~~~~are~~ estimated from approximately 700 $1^\circ \times 1^\circ$ ~~grid~~~~grid cells~~ over ~~that~~ cover
 1577 China. ~~Median~~ The median values (~~color~~~~coloured~~ dots with error bars of spatial
 1578 standard deviations) of ~~the trend biases in~~~~biases in the trends in~~ T_a (unit: $^\circ\text{C}/\text{decade}$)
 1579 in the twelve reanalyses ~~were~~~~are~~ regressed onto those of (a) the surface incident solar
 1580 radiation (R_s , unit: $\text{W m}^{-2}/\text{decade}$), (b) ~~precipitation frequency~~~~the frequency of~~
 1581 ~~precipitation~~~~precipitation frequency~~ (unit: days/decade) and (c) the surface downward
 1582 longwave radiation (L_d , unit: $\text{W m}^{-2}/\text{decade}$), using ~~the~~ ordinary least squares method
 1583 (OLS, denoted by ~~the~~ dashed grey lines) and ~~the~~ weighted total least squares method
 1584 (WTLS, denoted by ~~the~~ solid black lines). The 5-95% confidence intervals of ~~the~~
 1585 regressed slopes ~~obtained by the use of using~~ WTLS ~~were~~~~are~~ shown as shading. The

1586 regressed correlations and slopes were shown as grey and black fonttext,
1587 respectively.